2014

The Origin and Biosynthesis of the Benzenoid Moiety of Ubiquinone (Coenzyme Q) in *Arabidopsis*

Anna Block
University of Nebraska–Lincoln, ablock2@unl.edu

Joshua R. Widhalm
Purdue University, jwidhalm@purdue.edu

Abdelhak Fatihi
University of Nebraska–Lincoln, abdou.fatihi@unl.edu

Rebecca E. Cahoon
University of Nebraska-Lincoln, rcahoon2@unl.edu

Yashitola Wamboldt
University of Nebraska - Lincoln, ywamboldt2@unl.edu

See next page for additional authors

Published in *The Plant Cell* 26 (2014), pp. 1938-1948; doi: http://dx.doi.org/10.1105/tpc.114.125807

Submitted March 27, 2014; revised April 15, 2014; accepted April 24, 2014; published online May 2014.

The Origin and Biosynthesis of the Benzenoid Moiety of Ubiquinone (Coenzyme Q) in *Arabidopsis*

Anna Block,[1] Joshua R. Widhalm,[2] Abdelhak Fatihi,[1] Rebecca E. Cahoon,[1] Yashitola Wamboldt,[1] Christian Elowsky,[1] Sally A. Mackenzie,[1] Edgar B. Cahoon,[1] Clint Chapple,[2] Natalia Dudareva,[2] and Gilles J. Basset [1]

1.Center for Plant Science Innovation, University of Nebraska–Lincoln, Lincoln, Nebraska 68588
2. Department of Biochemistry, Purdue University, West Lafayette, Indiana 47907

Corresponding author – Gilles J. Basset, email gbasset2@unl.edu

Abstract
It is not known how plants make the benzenoid ring of ubiquinone, a vital respiratory cofactor. Here, we demonstrate that *Arabidopsis thaliana* uses for that purpose two separate biosynthetic branches stemming from phenylalanine and tyrosine. Gene network modeling and characterization of T-DNA mutants indicated that acyl-activating enzyme encoded by *At4g19010* contributes to the biosynthesis of ubiquinone specifically from phenylalanine. CoA ligase assays verified that At4g19010 prefers *para*-coumarate, ferulate, and caffeate as substrates. Feeding experiments demonstrated that the *at4g19010* knockout cannot use *para*-coumarate for ubiquinone biosynthesis and that the supply of 4-hydroxybenzoate, the side-chain shortened version of *para*-coumarate, can bypass this blockage. Furthermore, a *trans*-cinnamate 4-hydroxylase mutant, which is impaired in the conversion of *trans*-cinnamate into *para*-coumarate, displayed similar defects in ubiquinone biosynthesis to that of the *at4g19010* knockout. Green fluorescent protein fusion experiments demonstrated that At4g19010 occurs in peroxisomes, resulting in an elaborate biosynthetic architecture where phenylpropanoid intermediates have to be transported from the cytosol to peroxisomes and then to mitochondria where ubiquinone is assembled. Collectively, these results demonstrate that At4g19010 activates the propyl side chain of *para*-coumarate for its subsequent β-oxidative shortening. Evidence is shown that the peroxisomal ABCD transporter (PXA1) plays a critical role in this branch.

Introduction

Ubiquinone (coenzyme Q) is a prenylated benzoquinone that serves as a vital electron and proton carrier in the respiratory chain of mitochondria and some bacteria (Nowicka and Kruk, 2010). It is made up of a redox active benzoquinone ring and a prenyl side chain (Figure 1). In plants as in fungi and vertebrates, it is now established that the synthesis of the prenyl moiety, its conjugation to the benzenoid ring, and the subsequent methylation of the latter on carbon 5 (Figure 1) all take place in mitochondria (Avelange-Macherel and Joyard, 1998; Okada et al., 2004; Ducluzeau et al., 2012).

In contrast, the origin of the benzenoid backbone is not known (Kawamukai, 2009). Indeed, not only have the cognate enzymes yet to be identified, but what is known about the biosynthesis of the ring of ubiquinone in non-plant organisms delineates a puzzling evolutionary pattern. For instance, in *Escherichia coli*, the ring of ubiquinone is made from 4-hydroxybenzoate, which comes from the direct aromatization of chorismate catalyzed by chorismate pyruvate-lyase or UbiC (Figure 1; Nichols and Green, 1992). However, this enzyme appears to be restricted to the eubacterial lineage (Clarke, 2000; Kawamukai, 2009; Pfaff et al., 2014).

The yeast *Saccharomyces cerevisiae* is able to derive the ring of ubiquinone from the folate precursor *para*-aminobenzoate (*p*ABA), which is prenylated and then deaminated (Figure 1; Pierrel et al., 2010). Yeast and other fungi can also make the ring of ubiquinone from 4-hydroxybenzoate, although none of the steps in this alternative pathway are known and the relative contribution of the *p*ABA and 4-hydroxybenzoate branches is difficult to estimate (Law et al., 1971; Marbois et al., 2010). Vertebrates cannot synthesize *p*ABA, but early radiotracer studies have shown that mammals incorporate the ring of phenylalanine and tyrosine into the benzenoid moiety of ubiquinone and that 4-hydroxybenzoate is a likely intermediate (Figure 1; Olson et al., 1963). Since vertebrates are able to convert phenylalanine into tyrosine, these two amino acids most likely belong to a single linear biosynthetic branch leading to 4-hydroxybenzoate (Figure 1; Olson et al., 1963; Clarke, 2000). As is the case for yeast, the vertebrate enzymes involved in the biosynthesis of 4-hydroxybenzoate have not been identified.

Flowering plants a priori do not convert phenylalanine into tyrosine, as they appear to lack phenylalanine-4-hydroxylase (Pribat et al., 2010). However, plants do synthesize *p*ABA (Quinlivan et al., 2003), suggesting that a *p*ABA route toward ubiquinone could operate in the green lineage as it does in fungi (Figure 1). There is also the possibility that plants have evolved the capacity to synthesize the ring of ubiquinone via an entirely different pathway from those of other eukaryotes.

In this study, we show that *Arabidopsis thaliana* derives the ring of ubiquinone from that of phenylalanine and tyrosine via two nonintersecting routes. We focused on the phenylalanine pathway, and combining gene network modeling, isotopic labeling, and reverse genetics identified two enzymes and one transporter involved in the formation of the benzenoid ring of ubiquinone from the metabolism of phenylpropanoids.

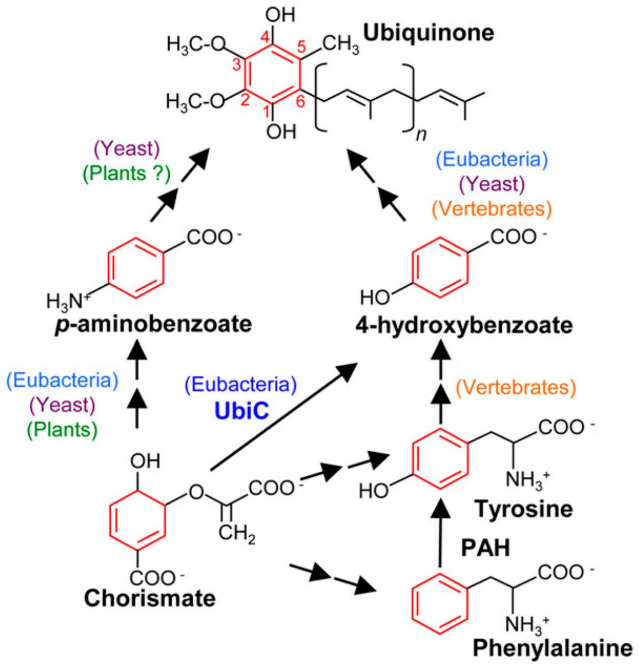

Figure 1. The Structure of Ubiquinone and the Metabolic Origin of Its Benzenoid Ring in *E. coli*, Yeast, and Vertebrates. Note that UbiC (chorismate-pyruvate lyase) occurs exclusively in eubacteria and that PAH (phenylalanine-4-hydroxylase) appears to be lacking in angiosperms.

Results

Arabidopsis Derives the Benzenoid Moiety of Ubiquinone from Phenylalanine and Tyrosine, Not from pABA

When axenic cultures of *Arabidopsis* were given identical doses of uniformly ^{13}C-labeled phenylalanine (Phe-[$^{13}C_9$]) or tyrosine (Tyr-[$^{13}C_9$;^{15}N]), ultraperformance liquid chromatography–electrospray ionization–tandem mass spectrometry analysis of the corresponding extracts readily detected the ion pairs characteristic of ubiquinone-[*Ring*-$^{13}C_6$] (Supplemental Figure 1). The isotopic enrichment of the benzoquinone ring was twice as high with Phe-[$^{13}C_9$] as with Tyr-[$^{13}C_9$;^{15}N] in both shoots and roots (Table 1). Importantly, ^{13}C isotopes of ubiquinone heavier than those labeled at the six ring positions were not detected, indicating that only the aromatic moiety of Phe-[$^{13}C_9$] and Tyr-[$^{13}C_9$;^{15}N] had been incorporated into ubiquinone. Because angiosperms appear to be unable to convert phenylalanine into tyrosine (Pribat et al., 2010), we inferred that the incorporation of these two aromatic amino acids into ubiquinone might occur, unlike in vertebrates, via two independent pathways. In stark contrast with yeast, *Arabidopsis* did not incorporate *p*ABA into ubiquinone (Table 1).

Gene Network Reconstruction Identifies a Functional Link between the Biosynthesis of Ubiquinone and a 4-Coumarate-CoA Ligase-Like in Arabidopsis

Mining the ATTED-II coexpression database (Obayashi et al., 2009) with genes involved in the assembly of the respiratory chain as queries detected gene *At4g19010* as a remarkable node interactor (Figure 2A). The cognate 57-kD protein features a conserved domain (cd05904) found in 4-coumarate-CoA ligases, and previous studies confirmed that recombinant At4g19010 displays CoA ligase activity with some hydroxycinnamate derivatives as substrates (Costa et al., 2005; Kienow et al., 2008). Two of *At4g19010*'s strongest interactors, *solanesyl-diphosphate synthase3* (*SPS3*; *At2g34630*), a *COQ1/lspB* ortholog, and *ABC transporter1* (*ABC1*; *At4g01660*), a *COQ8/UbiB* ortholog (Figure 2A), encode for enzymes involved in the biosynthesis of ubiquinone (Cardazzo et al., 1998; Ducluzeau et al., 2012; Block et al., 2013). Expanding the network reconstruction to the top 250 genes that coexpress with *At4g19010*, *SPS3*, and *ABC1* revealed that *At4g19010* shares 38% of its interactors with *SPS3* and/or *ABC1* (Figure 2B). Of those, 65% are shared uniquely with *SPS3*, 13% uniquely with *ABC1*, and 22% with both *SPS3* and *ABC1* (Figure 2B). It thus appears that the function of *At4g19010* is intimately connected to the mitochondrial electron and proton transport chain and more specifically to ubiquinone biosynthesis. It should also be noted that At4g19010 displays a C-terminal SerArgLeu tripeptide typifying a peroxisomal targeting signal-1; we will come back to this point later.

At4g19010 Contributes to the Formation of the Ring of Ubiquinone from Phenylalanine, but Not from Tyrosine

Two mutants corresponding to T-DNA insertions located in the first exon (SK_29455) and fifth intron (SALK_043310) of *At4g19010*, respectively, were identified using the T-DNA Express gene mapping tool of the SALK Institute (Figure 3A) and confirmed by DNA genotyping. RT-PCR analyses demonstrated that the insertion in line SK_29455 resulted in a knockdown mutation, while that of line SALK_043310 corresponded to a genuine knockout (Figure 3B). Both T-DNA lines were visually indistinguishable from wild-type plants. However, quantification of ubiquinone showed that its levels correlated with the expression of *At4g19010*; lines SK_29455 and SALK_043310 displaying 21 and 62% decrease in ubiquinone content com-

Table 1. Ubiquinone-[*Ring*$^{13}C_6$] Levels in *Arabidopsis*

	Ubiquinone-[*Ring*$^{13}C_6$], pmole· g^{-1} FW		
	Phe-[$^{13}C_9$]	Tyr-[$^{13}C_9$;^{15}N]	*p*ABA-[$^{13}C_6$]
Shoots	13 ± 2	6 ± 1	n.d.
Roots	12 ± 21	54 ± 13	n.d.

Data are means of three biological replicates 6 SE. n.d., not detected; FW, fresh weight.

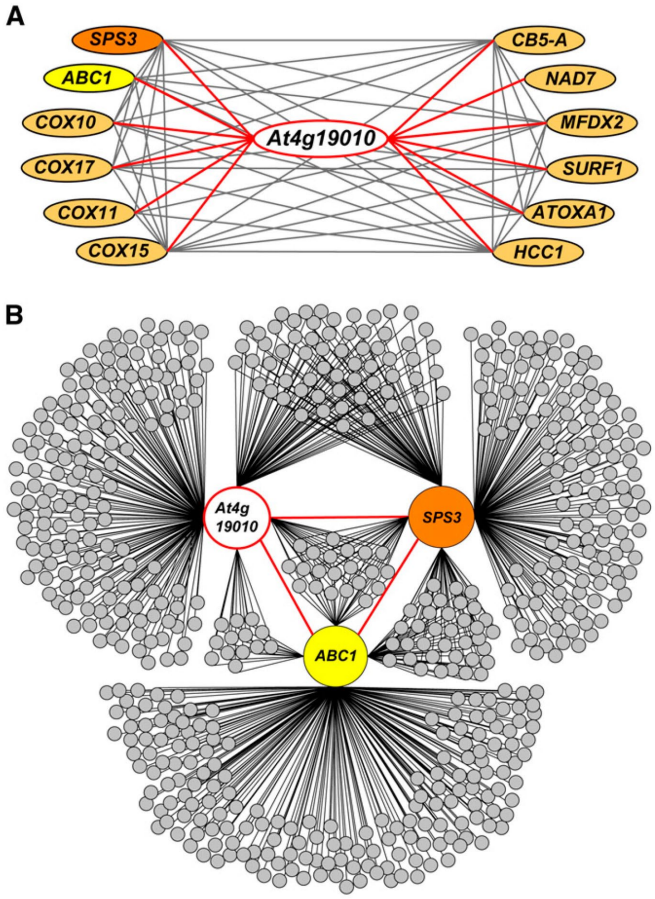

Figure 2. Gene Functional Network of *At4g19010*. **(A)** Interaction network reconstituted from the top 4.5% elements of the 22,263 expressed loci of the ATTED-II database that coexpress with the respiratory genes *SPS3*, *ABC1*, *COX10*, *COX17*, *COX11*, *COX15*, *CB5-A*, *NAD7*, *MFDX2*, *SURF1*, *OXA1*, and *HCC1*. **(B)** Reconstruction of the top 250 coexpressors of *At4g19010*, *SPS3*, and *ABC1*. The annotated lists of these genes and the correlation ranks of the latter are given in Supplemental Data Set 1.

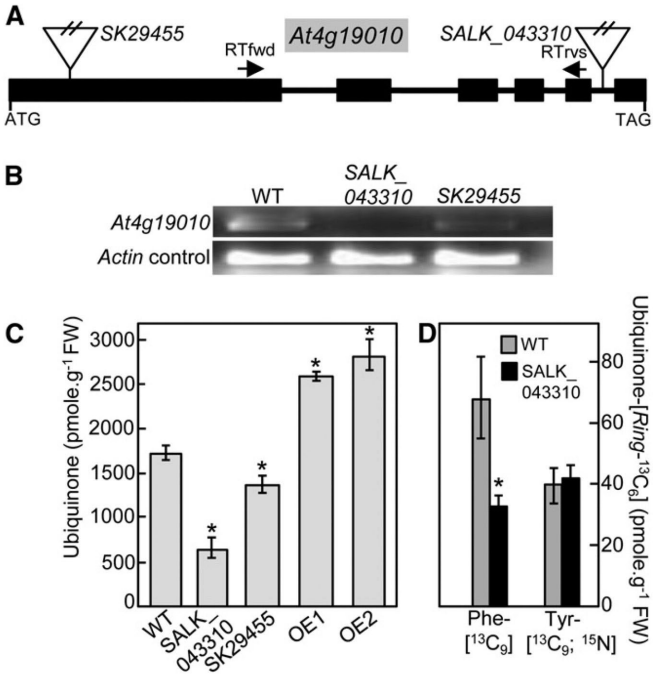

Figure 3. *At4g19010* Is Involved in the Biosynthesis of the Ring of Ubiquinone from Phenylalanine. **(A)** Structure of the *At4g19010* locus and location of the SALK_043310 and SK29455 insertions. Boxes and lines represent exons and introns, respectively. RTfwd and RTrvs indicate the location of the RT-PCR primers. **(B)** RT-PCR analyses of RNA abundance in wild-type and *at4g19010* plants showing that SALK_043310 is a knockout mutant and that SK29455 is a knockdown mutant. **(C)** Total ubiquinone (reduced and oxidized) levels in the leaves of wild-type plants, SALK_043310 knockout and SK29455 knockdown T-DNA mutants, and *At4g19010* overexpressing line OE1 and OE2. FW, fresh weight. **(D)** Total ubiquinone-[*Ring*-$^{13}C_6$] levels in axenically grown wild-type and SALK_043310 *Arabidopsis* plants fed with 250 µM doses of Phe-[$^{13}C_9$] or Tyr-[$^{13}C_9$;^{15}N] for 3 h. Data in **(C)** and **(D)** are means of four biological replicates ± se. Asterisk annotations indicate significant difference from the wild type as determined by Fisher's test ($P < \alpha = 0.05$) from an analysis of variance.

pared with wild-type plants, respectively (Figure 3C). Similarly, overexpression of *At4g19010* cDNA in two independent *Arabidopsis* transgenic lines resulted in the accumulation of ubiquinone to ~155% of wild-type content (Figure 3C). Furthermore, when Phe-[$^{13}C_9$] was fed to the *at4g19010* knockout, the isotopic enrichment of ubiquinone-[*Ring*-$^{13}C_6$] was half of that found in the wild-type control (Figure 3D). On the other hand, no statistically significant difference in ^{13}C isotope incorporation was observed between knockout and wild-type plants when Tyr-[$^{13}C_9$,^{15}N] was given to the plants (Figure 3D). All together these results demonstrate that *At4g19010* is involved in the biosynthesis of the benzenoid moiety of ubiquinone via the phenylalanine route.

In Vitro Activities of At4g19010

Previous investigations of the in vitro substrate preference of acyl activating enzymes reported conflicting data for At4g19010: one study mentioning marginal activity with caffeate and ferulate only (Costa et al., 2005), while a later study showed that the enzyme possessed conspicuous activity with *t*-cinnamate, *p*-coumarate, caffeate, and ferulate as well as with various aliphatic acids (Kienow et al., 2008). To clarify this point, an N-terminally 6xhis-tagged version of At4g19010 was codon-optimized for expression in *E. coli*, purified, and assayed using a standard spectrophotometric method with CoA, ATP, and *t*-cinnamate, *p*-coumarate, ferulate, caffeate, sinapate, 4-hydroxybenzoate, or acetate as substrates. CoA ligase activity was readily detected with *t*-cinnamate, *p*-coumarate, ferulate, and caffeate, allowing further investigation of At4g19010's kinetic properties. K_m, k_{cat}, and k_{cat}/K_m values determined with *p*-coumarate, ferulate, and caffeate were similar (Table 2). The catalytic efficiency of the enzyme with *t*-cinnamate was only 20 to 35% of that mea-

sured with *p*-coumarate, ferulate, or caffeate, owing to a lower k_{cat} value with this substrate (Table 2). Overall, the kinetic parameters of At4g19010 determined with *t*-cinnamate, *p*-coumarate, ferulate, and caffeate were similar to those previously reported for plant *p*-coumarate and *t*-cinnamate-CoA ligases (Ehlting et al., 1999; Hamberger and Hahlbrock, 2004; Klempien et al., 2012). Notably, as is usually observed for *p*-coumarate-CoA ligases (Ehlting et al., 1999; Hamberger and Hahlbrock, 2004), no activity was detected with sinapate, the ring of which is methoxylated on C5, while *t*-cinnamate, *p*-coumarate, ferulate, and caffeate are unsubstituted at this position (Table 2). Anecdotal catalytic efficiency was found with 4-hydroxybenzoate, while no activity could be detected with acetate (Table 2). These data thus verify that recombinant At4g19010 is predominantly active with *t*-cinnamate, *p*-coumarate, ferulate, and caffeate, although they say nothing about which of these substrates might actually play a role in ubiquinone biosynthesis in vivo. Assays with plant extracts did not show any statistically significant difference in CoA ligase activity between wild-type and *at4g19010* knockout plants (Supplemental Table 1).

t-Cinnamate, *p*-Coumarate, and 4-Hydroxybenzoate Serve as Ubiquinone Precursors

To gain some insight into the architecture of the metabolic branch of which At4g19010 belongs to, ubiquinone levels were determined in wild-type and *at4g19010* knockout plants fed with *t*-cinnamate (the product of phenylalanine ammonia lyase), *p*-coumarate, ferulate, or caffeate, or with their corresponding shortened aliphatic side-chain versions, i.e., benzoate, 4-hydroxybenzoate, vanillate, or 3,4-dihydroxybenzoate, respectively (Figure 4A). Feeding wild-type plants with *t*-cinnamate, *p*-coumarate, and 4-hydroxybenzoate increased ubiquinone content by ~30% compared with the DMSO control, whereas only 4-hydroxybenzoate restored ubiquinone biosynthesis in the *at4g19010* knockout (Figure 4B). Because *t*-cinnamate is the immediate precursor of *p*-coumarate (Schilmiller et al., 2009) and plants are able to derive 4-hydroxybenzoate from *p*-coumarate (Löscher and Heide, 1994), our results strongly suggest that *t*-cinnamate, *p*-coumarate, and 4-hydroxybenzoate are used as precursors of ubiquinone via the same metabolic branch. That ubiquinone biosynthesis in the *at4g19010* knockout is rescued exclusively by 4-hydroxybenzoate would therefore indicate that the loss of function of At4g19010 creates a metabolic blockage upstream of 4-hydroxybenzoate and downstream of *t*-cinnamate and *p*-coumarate. Agreeing with such a model, an *Arabidopsis reduced epidermal fluorescence3-2* (*ref3-2*) leaky mutant that displays reduced cinnamate 4-hydroxylase activity and is thus impaired in its ability to convert *t*-cinnamate into *p*-coumarate (Schilmiller et al., 2009) contained only 40% of wild-type ubiquinone level (Figure 4C) and displayed a 75% decrease in isotopic enrichment of ubiquinone-[*Ring*-$^{13}C_6$] from Phe-[$^{13}C_9$] (Figure 4C). As observed for the *at4g19010* knockout, the incorporation of Tyr-[$^{13}C_9$;^{15}N] into ubiquinone in the *ref3-2* mutant remained intact (Figure 4C). Taken together, these results are consistent with At4g19010 operating as a CoA ligase that activates the propyl side chain of *p*-coumarate for its subsequent β-oxidative shortening, leading to 4-hydroxybenzoate.

At4g19010 Is Localized in Peroxisomes

Homology searches across terrestrial plant lineages showed that the putative orthologs of At4g19010 display the hallmark stringent conservation of an authentic peroxisomal targeting sequence-1 (Figure 5A). Coexpression experiments in *Nicotiana benthamiana* mesophyll cells confirmed that the green pseudocolor of the green fluorescent protein (GFP) fused to the N terminus of At4g19010 strictly colocalized with the red pseudocolor of a red fluorescent protein (RFP)–tagged fragment of 3-keto-acyl-CoA thiolase 2 in peroxisomes (Figure 5B). Control coexpression of the GFP-At4g19010 fusion protein with RFP-tagged isovaleryl-CoA dehydrogenase verified that the fluorescence of GFP was not associated with mitochondria (Figure 5C). That At4g19010 is localized in peroxisomes, while cinnamate-4-hydroxylase is bound to the endomembrane system in the cytosol (Achnine et al., 2004), implies that *p*-coumarate might be transported into peroxisomes. Reexamination of the *At419010/SPS3/ABC1* functional network identified the peroxisome ABC subfamily D transporter 1 or *PXA1* (Zolman et al., 2001) as one of the interacting genes shared between *At4g19010* and *SPS3* (rank 214 and 291, respectively; Supplemental Data Set 1). Quinone analysis showed that the *pxa1* knockout contained 55% less ubiquinone than the wild-type control and that as observed for the *at4g19010* and *ref3-2* mutants, such a loss was exclusively attributable to a decrease in biosynthetic flux from phenylalanine (Figures 6A and 6B). Feeding experiments showed that of *t*-cinnamate, *p*-coumarate, and 4-hydroxybenzoate, only the latter rescued ubiquinone biosynthesis in the *pxa1* knockout, demonstrating that here again the metabolic blockage occurred between *p*-coumarate and 4-hydroxybenzoate (Figure 6C). Further verifying that the impact of the *pxa1* mutation on quinone metabolism

Table 2. Kinetic Properties of Recombinant At4g19010

	K_m (μM)	k_{cat} (s^{-1})	k_{cat}/K_m (s^{-1}, mM^{-1})	
t-Cinnamate	112 ± 37	0.7 ± 0.2	6 ± 2	
p-Coumarate	125 ± 25	2.1 ± 0.4	17 ± 3.4	
Ferulate	113 ± 45	3.6 ± 1.4	32 ± 13	
Caffeate	85 ± 12	2.4 ± 0.3	28 ± 4	
Sinapate	n.d.	n.d.	n.d.	
4-Hydroxybenzoate	67 ± 30	0.01 ± 0.01	0.15 ± 0.07	
Acetate	n.d.	n.d.	n.d.	

Data are means of six experimental replicates from two enzyme purifications ± SE. n.d., not determined, for no activity was detected at any of the substrate concentrations tested.

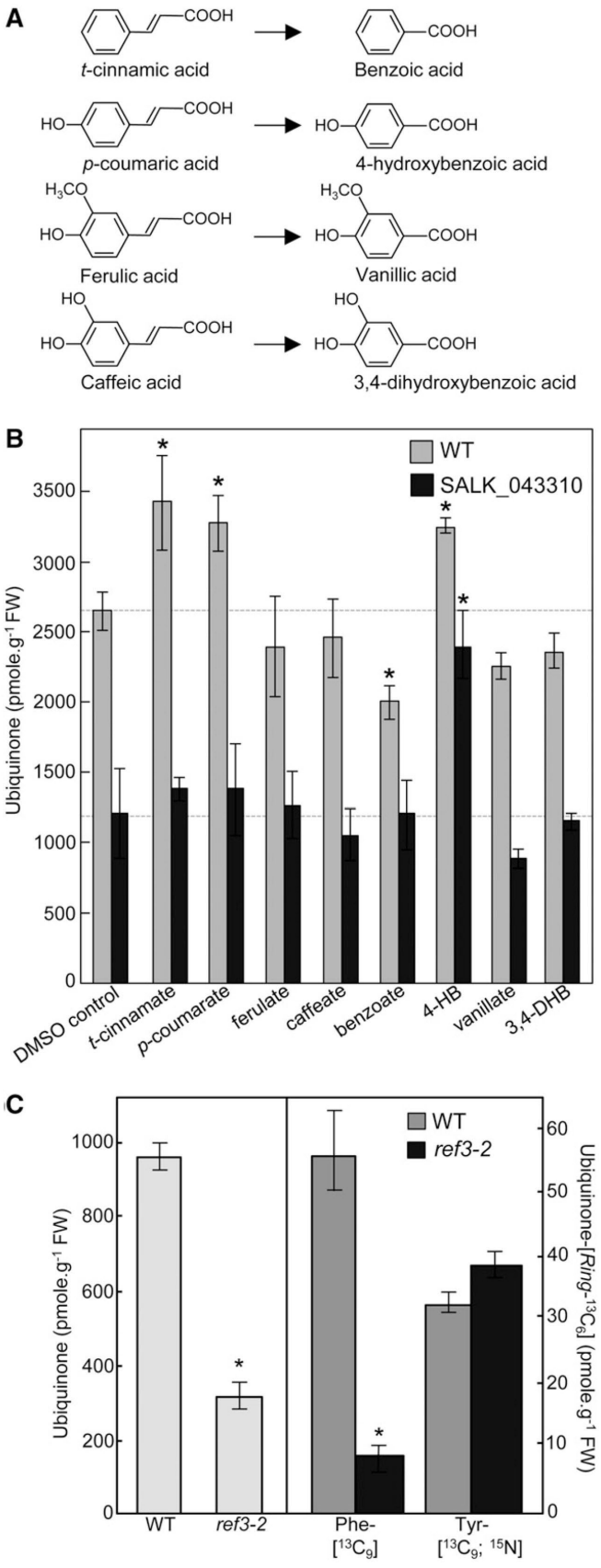

is specific to ubiquinone biosynthesis, no statistically significant difference in the levels of phylloquinone, the naphthoquinone ring of which is made in part in peroxisomes (Reumann, 2013), was observed between the *pxa1* mutant and the wild-type control (Figure 6D).

Discussion

Plant Peroxisomes Contribute to the Biosynthesis of Ubiquinone

Despite the role of ubiquinone as a crucial cofactor for respiration, the metabolic origin of its benzenoid ring has long remained enigmatic in most eukaryotes (Clarke, 2000; Kawamukai, 2009). One might assume that since plants synthesize *p*ABA de novo (Quinlivan et al., 2003), they could use this metabolite for the biosynthesis of ubiquinone as yeast does (Marbois et al., 2010; Pierrel et al., 2010). Our data show that this is not so, most probably because, unlike yeast, plant cells sequester *p*ABA as a glucose ester conjugate and thus have a minute pool of the free acid form (Quinlivan et al., 2003). Collectively, our data demonstrate that plants have evolved instead the capacity to derive the benzenoid moiety of ubiquinone from the β-oxidative metabolism of phenylpropanoids, adding de facto respiration to the core cellular processes that depend upon plant peroxisomes. Such an arrangement results in an elaborate biosynthetic architecture, in which intermediates are trafficked between the cytosol, where *p*-coumarate is made (Achnine et al., 2004), peroxisomes, where this study shows that *p*-coumarate is activated by ligation with CoA for its subsequent shortening into 4-hydroxybenzoate, and mitochondria, where the latter is prenylated and modified (Avelange-Macherel and Joyard, 1998; Okada et al., 2004; Ducluzeau et al., 2012). A proposed scheme of the cognate metabolic branches and their respective compartmentation is shown in Figure 7. A compelling parallel can actually be drawn between our finding that the peroxisome transporter PXA1 participates in this trafficking and the earlier report that PXA1 is required for the β-oxidative activation of the protoherbicide 2,4-dichlorophenoxybutyric acid into 2,4-D (Footitt et al., 2002). Indeed,

Figure 4. *t*-Cinnamate, *p*-Coumarate, and 4-Hydroxybenzoate Serve as Precursors of Ubiquinone in *Arabidopsis*. **(A)** Structures of *t*-cinnamic, *p*-coumaric, ferulic and caffeic acids, and their corresponding shortened aliphatic side-chain versions. **(B)** Total ubiquinone (reduced and oxidized) levels in axenically grown wild-type and SALK_043310 *Arabidopsis* plants fed for 24 h with 200 μM *t*-cinnamate, *p*-coumarate, ferulate, caffeate, benzoate, 4-hydroxybenzoate (4-HB), vanillate, or 3,4-dihydroxybenzoate (3,4-DHB). Data are means of four biological replicates ± se. Asterisk annotations indicate significant difference from the corresponding DMSO control as determined by Fisher's test ($P < \alpha = 0.05$) from an analysis of variance. FW, fresh weight. **(C)** Left panel, total ubiquinone levels in the leaves of the wild type and cinnamate-4 hydroxylase mutant (*ref3-2*) *Arabidopsis* plants. Right panel, total ubiquinone-[*Ring*-$^{13}C_6$] levels in axenically grown wild-type and *ref3-2 Arabidopsis* plants fed with 250 μM doses of Phe-[$^{13}C_9$] or Tyr-[$^{13}C_9$,^{15}N] for 3 h. Data are means of four biological replicates ± se. Asterisk annotations indicate significant difference from the wild type as determined by Fisher's test ($P < \alpha = 0.05$) from an analysis of variance.

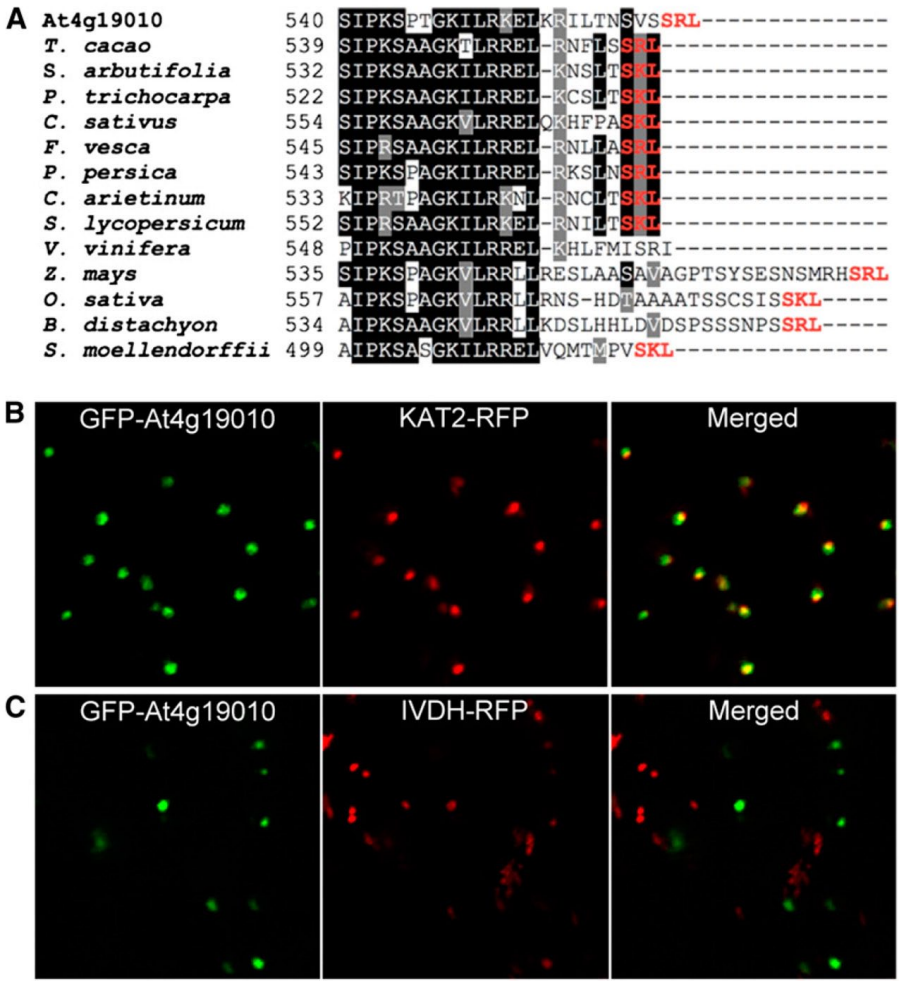

Figure 5. Subcellular Localization of At4g19010. **(A)** Alignment of the C-terminal regions of At4g19010 and its orthologs in cacao tree (*Theobroma cacao*), willow (*Salix arbutifolia*), poplar (*Populus trichocarpa*), cucumber (*Cucumis sativus*), strawberry (*Fragaria vesca*), peach (*Prunus persica*), chickpea (*Cicer arietinum*), tomato (*Solanum lycopersicum*), grape vine (*Vitis vinifera*), maize (*Zea mays*), rice (*Oryza sativa*), *Brachypodium distachyon*, and *Selaginella moellendorffii*. The tripeptides corresponding to consensus peroxisomal targeting sequence-1 are highlighted in red. Identical residues are shaded in black and similar ones in gray. Dashes symbolize gaps introduced to maximize alignment. **(B)** Left panel, green pseudocolor of GFP fused to the N terminus of At4g19010; center panel, red pseudocolor of peroxisomal marker RFP-tagged 3-keto-acyl-CoA thiolase 2 (KAT2); right panel, overlay. **(C)** Left panel, green pseudocolor of GFP fused to the N terminus of At4g19010; center panel, red pseudocolor of mitochondrial marker RFP-tagged isovaeryl-CoA dehydrogenase (IVDH); right panel, overlay.

while wild-type *Arabidopsis* is sensitive to both 2,4-dichlorophenoxybutyric acid and 2,4-D, the *pxa1* knockout is unable to β-oxidize 2,4-dichlorophenoxybutyric acid and is sensitive only to 2,4-D (Footitt et al., 2002). Similarly, our data show that ubiquinone biosynthesis in the *pxa1* knockout is restored by 4-hydroxybenzoate, but not by its parent compound *p*-coumarate. Furthermore, the recent demonstration that PXA1 displays acyl-CoA thioesterase activity (De Marcos Lousa et al., 2013), raises the question of whether the cytosolic pool of *p*-coumaryl-CoA contributes to ubiquinone biosynthesis.

The Function of At4g19010 in Ubiquinone Biosynthesis Is That of a p-Coumarate-CoA Ligase

At4g19010 belongs to clade V of the plant superfamily of acyl-activating enzymes, the respective cellular functions of which have been so far particularly difficult to attribute due to their general lack of substrate specificity in vitro (Kienow et al., 2008; Shockey and Browse, 2011). In fact, besides At4g19010, only one out of eight clade V *Arabidopsis* members, *At1g20510*, which encodes for 3′-oxo-2-(2′-[*Z*]-pentenyl) cyclopentane-1-octanoic acid CoA ligase 1 (OPCL1) of the jasmonate biosynthetic pathway, has a known physiological role (Koo et al., 2006). In vitro, OPCL1 is as active with C8-C18 aliphatic acids as it is with 3′-oxo-2-(2′-[*Z*]-pentenyl) cyclopentane-1-octanoic acid, its authentic in vivo substrate (Kienow et al., 2008). Similarly, At1g20500, another class V member, displays as much activity with sinapate as it does with the structurally unrelated jasmonate precursor 3′-oxo-2-(2′-[*Z*]-pentenyl) cyclopentane-1-hexanoic acid (Kienow et al., 2008). Therefore, it is clear that the in vivo function of class V acyl activating enzymes cannot be inferred from their substrate preference alone. In this study, we present three lines of evidence

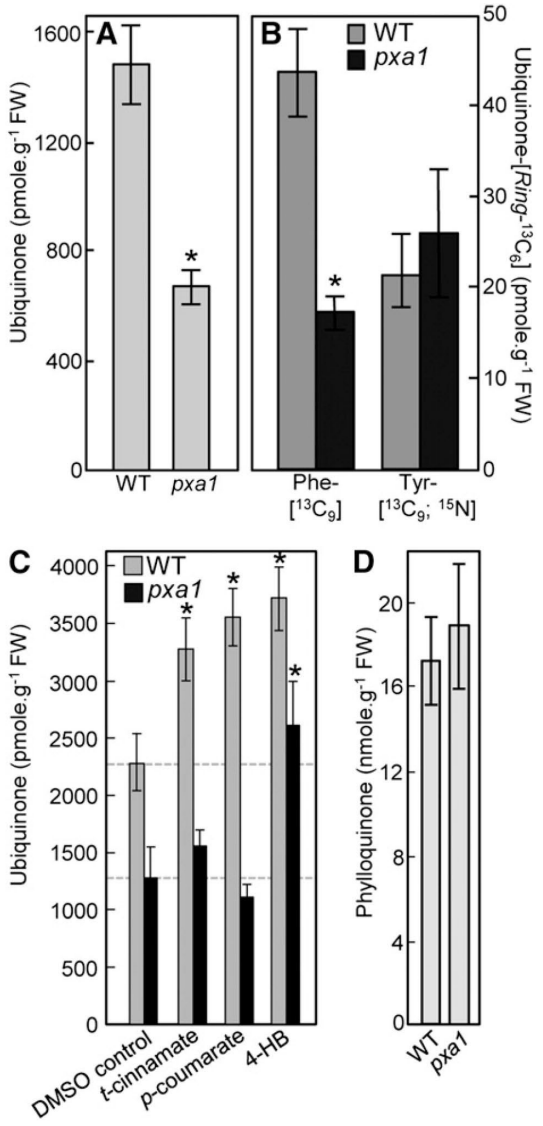

Figure 6. The Peroxisomal Transporter PXA1 Is Involved in Ubiquinone Biosynthesis from Phenylalanine. **(A)** Total ubiquinone (reduced and oxidized) levels in the leaves of wild-type and *pxa1* knockout *Arabidopsis* plants. Data are means of four biological replicates ± se. Asterisk annotations indicate significant difference from the wild type as determined by Fisher's test ($P < \alpha = 0.05$) from ANOVA. FW, fresh weight. **(B)** Total ubiquinone-[*Ring*-$^{13}C_6$] levels in axenically grown wild-type and *pxa1* knockout *Arabidopsis* plants fed with 100 µM doses of Phe-[$^{13}C_9$] or Tyr-[$^{13}C_9$,^{15}N] for 3 h. Data are means of four biological replicates ± se. Asterisk annotations indicate significant difference from the wild type as determined by Fisher's test ($P < \alpha = 0.05$) from ANOVA. **(C)** Total ubiquinone levels in axenically grown wild-type and *pxa1* knockout *Arabidopsis* plants fed for 24 h with 200 µM *t*-cinnamate, *p*-coumarate, or 4-hydroxybenzoate (4-HB). Data are means of three to five biological replicates ± se. Asterisk annotations indicate significant difference from the corresponding DMSO control as determined by Fisher's test ($P < \alpha = 0.05$) from ANOVA. **(D)** Phylloquinone levels in the leaves of wild-type *pxa1 Arabidopsis* plants. Data are means of three biological replicates ± se. Wild-type and *pxa1* values are not significantly different as determined by Fisher's test from ANOVA ($P > 0.4$).

indicating that the role of At4g19010 in ubiquinone biosynthesis is that of a *p*-coumarate-CoA ligase. First, the usage of *p*-coumarate as a precursor for ubiquinone biosynthesis is blocked in the *at4g19010* knockout. Second, this blockage can be bypassed exclusively by the exogenous supply of 4-hydroxybenzoate, the β-oxidized product of *p*-coumarate. Last, recombinant At4g19010 catalyzes the conversion of *p*-coumarate into *p*-coumaroyl-CoA with similar catalytic efficiency to that of previously characterized *p*-coumarate-CoA ligases, while as is generally observed for this class of enzymes, At4g19010 is not active with sinapate (Ehlting et al., 1999; Hamberger and Hahlbrock, 2004).

β-Oxidation of Phenylpropanoids Is a Common Mechanism in the Biosynthetic Pathways of Benzenoid-Derived Compounds

The β-oxidative shortening of *p*-coumarate is reminiscent of that of *t*-cinnamate, which undergoes a similar route in the biosynthetic pathways of benzoyloxyglucosinolates, xanthone phytoalexin, and benzenoid floral volatiles (Kliebenstein et al., 2007; Colquhoun et al., 2012; Gaid et al., 2012; Klempien et al., 2012; Lee et al., 2012; Bussell et al., 2014). The conversion of *p*-coumaryl-CoA into 4-hydroxybenzoate requires four yet to be identified steps, i.e., those corresponding to the hydration, dehydrogenation, and thiolation of the β-oxidative cycle followed by the final hydrolysis of the 4-hydroxybenzoyl-CoA thioester. A prime *Arabidopsis* candidate for the hydration and dehydrogenation steps is the bifunctional peroxisomal enzyme AIM1 (Richmond and Bleecker, 1999), the petunia (*Petunia hybrida*) ortholog of which was recently shown to participate in the β-oxidative shortening of cinnamoyl-CoA into benzoic acid and to be also active with *p*-coumaroyl-CoA (Qualley et al., 2012). Similarly, peroxisomal thiolases and CoA thioesterases that act on benzenoid substrates have recently been identified in plants (Van Moerkercke et al., 2009; Widhalm et al., 2012). Plant peroxisomes thus appear to contain the necessary core enzymatic machinery to complete the β-oxidation of *p*-coumaroyl-CoA to 4-hydroxybenzoate.

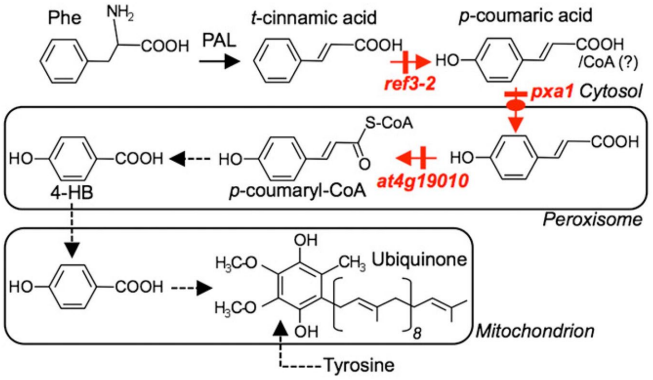

Figure 7. Architecture of 4-Hydroxybenzoic Acid Biosynthesis from Phenylalanine in Relation to Ubiquinone Biosynthesis. The Arabidopsis mutants investigated in this study are indicated in red. Dashed arrows denote multiple steps. 4-HB, 4-hydroxybenzoic acid; PAL, phenylalanine ammonia lyase.

Plants Possess a Second Route to Synthesize the Ring of Ubiquinone

It is clear from our data that phenylalanine supplies approximately half of ubiquinone biosynthetic flux and that plants can also use tyrosine to make the ring of ubiquinone. That the *at4g19010*, *ref3-2*, and *pxa1* mutants have fully retained the capacity to incorporate the benzenoid skeleton of tyrosine into ubiquinone indicates that this alternate route does not intersect with that originating from phenylalanine. Interestingly, the biosynthesis of terpenoid benzoquinones in plastids provides an evolutionary instance of tyrosine serving as a ring precursor via a non-β-oxidative route (DellaPenna and Pogson, 2006). In this pathway, tyrosine is first deaminated into 4-hydroxyphenylpyruvate, which is then decarboxylated and hydroxylated with concomitant migration of the side chain, yielding homogentisate (Supplemental Figure 2). The loss of a second carbonyl occurs simultaneously with the prenylation of homogentisate (Supplemental Figure 2). Future investigations will examine the possible occurrence of metabolic branch-points from 4-hydroxyphenylpyruvate and homogentisate toward ubiquinone.

Methods

Bioinformatics

Protein and gene sequences were retrieved from the National Center for Biotechnology Information database (http://www.ncbi.nlm.nih.gov). Protein sequences were aligned using MultAlin (http://multalin.toulouse.inra.fr/multalin/). Orthology was determined using phylogeny.fr (http://www.phylogeny.fr). Gene networks were reconstructed by mining coexpressors from the ATTED-II database (http://atted.jp) using *Arabidopsis thaliana* respiratory genes as queries. Coexpressing genes were then aggregated using GeneVenn (http://genevenn.sourceforge.net).

Chemicals and Reagents

p-Aminobenzoic acid-[$^{13}C_6$] was from IsoSciences, l-phenylalanine-[$^{13}C_9$], and l-tyrosine-[$^{13}C_9$,^{15}N] were from Cambridge Isotope Laboratories. *t*-Cinnamic and benzoic acids and their hydroxyl/methoxy derivatives were from Sigma-Aldrich. Unless mentioned otherwise, other reagents were from Fisher Scientific.

Plant Material and Growth Conditions

Arabidopsis SALK_043310 (Alonso et al., 2003) and SK_29455 (Robinson et al., 2009) insertion lines, as well as the *pxa1* ethyl methanesulfonate mutant (Zolman et al., 2001; stock number CS3950), were obtained from the ABRC. The *ref3-2* mutant was generated and identified in the laboratory of one of the coauthors (C.C.) as previously described (Schilmiller et al., 2009). Seeds were germinated on Murashige and Skoog solid medium, transferred to soil, and then grown at 22°C in 16-h days (110 μE m^{-2} s^{-1}) for 4 weeks. For feeding experiments, plants were germinated and grown in Murashige and Skoog liquid medium containing sucrose (10 g/liter) on an orbital shaker (60 rpm) in 10-h days (200 μE m^{-2} s^{-1}) at 22°C.

RT-PCR Analyses

Total leaf RNA was extracted using the RNeasy plant mini kit (Qiagen). cDNAs were then prepared from total RNA (500 ng) using the ImProm-II reverse transcription system (Promega). PCR amplification was performed on a 3Prime thermal cycler (Techne) using the following gene-specific primer pairs: *At4g19010*, 5′-GGAGTTTGTGGTGAAGTGTTT-3′ and 5′-CAAGGGATGTGAAACAAGAAC-3′; actin control, 5′-CTAAGCTCTCAAGATCAAAGGC-3′ and 5′-TTAACATTGCAAAGAGTTTCAAGG-3′.

Preparation of Recombinant At4g19010 and Plant Extracts

Full-length *At4g19010* cDNA (ABRC clone G60335) was codon optimized (GenScript) and subcloned using Gateway technology into expression vector pDEST17 (Invitrogen) for N-terminal fusion with a 6xHis tag. This construct was introduced in *Escherichia coli* BL21 Star (DE3) pLysS (Invitrogen). Protein expression was induced in Luria-Bertani medium with 0.5 mM isopropyl β-d-1-thiogalactopyranoside for 16 h at 20°C. Cells were harvested by centrifugation and disrupted in 50 mM NaH_2PO_4 (pH 8.0), 300 mM NaCl, 10 mM imidazole, and 0.1% (v/v) Triton X-100 using 0.1-mm Zirconia/silica beads in a MiniBeadbeater (BioSpec Products). The extract was cleared by centrifugation, and the recombinant protein was purified under native conditions with Ni-NTA His-Bind resin (Novagen) following the manufacturer's recommendations. The isolated enzyme was desalted on a PD-10 column equilibrated in 100 mM KH_2PO_4 (pH 8.0), 10% (v/v) glycerol, and 5 mM $MgCl_2$. The desalted enzyme was frozen in liquid N_2 and stored at −80°C. Negative controls consisting of untransformed BL21 Star (DE3) pLysS cells were processed in parallel. For the preparation of plant extracts, *Arabidopsis* leaves (1 g) were ground into a fine powder using a mortar and pestle under liquid N_2. The powder was then thawed in 5 mL of 100 mM KH_2PO_4 (pH 8.0), 10% (v/v) glycerol, 5 mM $MgCl_2$, 1% (v/v) of β-mercaptoethanol, and 5% (w/v) of cross-linked poly vinylpyrrolidone. Extracts were centrifuged (10,000*g* for 10 min at 4°C) to pellet the cell debris and the supernatants immediately desalted on a PD-10 column equilibrated in 100 mM KH_2PO_4 (pH 8.0), 10% (v/v) glycerol, and 5 mM $MgCl_2$. Desalted fractions were dispensed into 500 μL aliquots, flash frozen in liquid N_2, and stored at −80°C. Protein concentration was quantified by the method of Bradford (Bradford, 1976) using BSA as a standard.

Enzyme Assays

Assays (1 mL) contained 100 mM KH_2PO_4 (pH 8.0), 10% (v/v) glycerol, 5 mM $MgCl_2$, 2.5 mM ATP, 0.5 mM CoA, 0 to 300 μM of organic acid, and 0 to 25 μg of protein. Reactions were performed for 30 to 60 min at 30°C. The increase in absorbance due to the formation of the CoA thioesters was monitored on an Agilent 8453 diode array spectrophotometer using the following wavelengths and molar extinction coefficients: 311 nm and 22,000 M^{-1} cm^{-1} for *t*-cinnamoyl-CoA, 333 nm and 21,000 M^{-1} cm^{-1} for *p*-coumaroyl-CoA, 345 nm and 19,000 M^{-1} cm^{-1} for feruloyl-CoA, 346 nm and 18,000 M^{-1} cm^{-1} for caffeoyl-CoA, 352 nm and 20,000 M^{-1} cm^{-1} for sinapoyl-CoA, 330 nm and 24,000 M^{-1} cm^{-1} for 4-hydroxybenzoyl-CoA, and 232 nm and 4500 M^{-1} cm^{-1} for acetyl-CoA (Dawson et al., 1986; Lee et al., 1997; Egland and Harwood, 2000).

Terpenoid Quinones Analyses

For ultraperformance liquid chromatography–electrospray ionization–tandem mass spectrometry analysis, ubiquinone was extracted as previously described (Ducluzeau et al., 2012), except that the reduction step with $NaBH_4$ was omitted. Reduced and oxidized ubiquinones were separated on an Eclipse Plus C18 column (Agilent Technologies) held at 40°C at a flow rate of 0.2 mL min^{-1} with a binary gradient system consisting of solvent A, methanol: isopropanol (80:20) + 10 mM ammonium acetate, and solvent B, isopropanol: hexane (60:40) + 10 mM ammonium acetate. An 8-min gradient was generated starting with 30% solvent B for 3 min and increased to 60% solvent B over 2 min and held at 60% for 1 min before returning to 30% B at 6.6 min. The eluate was directed to a TurboV ion source of the 4000 QTRAP triple quadrupole mass spectrometer operated in positive mode at +5000 V. The temperature was held at 200°C, nebulizing gas (GS1) was set at 16 p.s.i., focusing gas (GS2) at 20 p.s.i., curtain gas at 20 p.s.i., and the interface heater was engaged. Declustering potential (40 V), collision energy (34 V), entrance potential (10 V), and collision exit potential (11 V) were optimized using a standard of ubiquinone-10. Reduced and oxidized ubiquinones were

measured by Multiple Reaction Monitoring using dwell times of 50 ms and the following ion pairs: ubiquinone-9 (812.8/197.1), ubiquinol-9 (814.8/197.1), ubiquinone-10 (880.8/197.1), ubiquinol-10 (882.8/197.1), ubiquinone-9-[$^{13}C_6$] (818.8/203.1), ubiquinol-9-[$^{13}C_6$] (820.8/203.1), ubiquinone-10-[$^{13}C_6$] (886.8/203.1), and ubiquinol-10-[$^{13}C_6$] (888.8/203.1). Retention times were 3.1 min for ubiquinol-9, 3.6 min for ubiquinol-10, 4.1 min for ubiquinone-9, and 5 min for ubiquinone-10. HPLC-diode array spectrophotometry analysis of total ubiquinones was performed as previously described (Ducluzeau et al., 2012). Phylloquinone levels were determined on the leaves of *Arabidopsis* plants grown on Murashige and Skoog medium containing sucrose using the HPLC-fluorescence method of Widhalm et al. (2012).

Subcellular Localization and Overexpression of At4g19010 in Arabidopsis

Full-length *At4g19010* cDNA was subcloned into pK7WGF2 (Karimi et al., 2002) using Gateway technology, resulting in an in-frame fusion of GFP to the N terminus of At4g19010. The KAT2-eqFP611 peroxisomal marker cassette, encoding for a fragment (residues 1 to 99) of *Arabidopsis* 3-keto-acyl-CoA thiolase 2 fused to the N-terminal end of RFP under the control of the 35S promoter (Forner and Binder, 2007), was subcloned into the *Eco*RI and *Pst*I sites of binary vector PZP212 (Hajdukiewicz et al., 1994). Vector pLN3639 allowed expression of the IVDH mitochondrial marker consisting of the N-terminal region of isovaleryl-CoA dehydrogenase fused to the N-terminal end of RFP under the control of the 35S promoter (Block et al., 2010). The 35S:GFP-*At4g19010* construct was electroporated into *Agrobacterium tumefaciens* C58C1 for subsequent coinfiltration into the leaves of *Nicotiana benthamiana* with a second strain harboring either PZP212-35S:KAT2-eqFP611 or pLN3639. Epidermal cells were imaged by confocal microscopy 48 h later using a Nikon A1 laser scanning microscope. GFP, RFP, and chlorophyll were excited and collected sequentially. Excitation wavelengths were 488 nm for GFP, 561 nm for RFP, and 641 nm for chlorophyll. Emissions were collected from 500 to 550 nm for GFP, 570 to 620 nm for RFP, and 663 to 738 nm for chlorophyll.

Stable Overexpression of At4g19010 in Arabidopsis

Full-length *At4g19010* cDNA was subcloned under the control of the 35S promoter in pB2GW7 (Karimi et al., 2002) using Gateway technology. This construct was introduced into *Arabidopsis* plants ecotype Columbia-0 using the floral dip method (Clough and Bent, 1998), and the resulting transgenics were selected on soil by spraying 100 mg L^{-1} of BASTA.

Accession Numbers

Sequence data from this article can be found in the GenBank/EMBL libraries under the following accession numbers: *At2g34630* (*SPS3*), *At4g01660* (*ABC1*), *At2g44520* (*COX10*), *At3g15352* (*COX17*), *At1g02410* (*COX11*), *At5g56090* (*COX15*), *At1g26340* (*CB5-A*), *AtMg00510* (*NAD7*), *At4g21090* (*MFDX2*), *At3g17910* (*SURF1*), *At5g62050* (*OXA1*), and *At3g08950* (*HCC1*). At4g19010 (AAO64847.1) and its orthologs EOY25276.1 (*T. cacao*), AGO89326.1 (*S. arbutifolia*), XP_002304364.1 (*P. trichocarpa*), XP_004144410.1 (*C. sativus*), XP_004301643.1 (*F. vesca*), EMJ05131.1 (*P. persica*), XP_004512448.1 (*C. arietinum*), XP_004245937.1 (*S. lycopersicum*), XP_002270360.1 (*V. vinifera*), DAA46521.1 (*Z. mays*), EAZ05563.1 (*O. sativa*), EAZ05563.1 (*B. distachyon*), and XP_002985111.1 (*S. moellendorffii*).

Supplemental Data

The following materials are available in the pages following this article.

Supplemental Figure 1. Extracted Counts of Ion Pairs for Multiple Reaction Monitorings of Ubiquinone Isotopes.

Supplemental Figure 2. Formation of the Ring of Plastid Prenyl Benzoquinones from Tyrosine.

Supplemental Table 1. CoA Ligase Activity in *Arabidopsis* Extracts.

Supplemental Data Set 1. Correlation Ranks and Functional Annotations of the Top 500 Coexpressors of *At4g19010*, *SPS3*, and *ABC1*.

Acknowledgments – This work was made possible in part by National Science Foundation Grants MCB-0918258, MCB-1148968 (to G.J.B.), and MCB-0919987 (to N.D.) and by the Gordon and Betty Moore Foundation through Grant GBMF2550.02 to the Life Sciences Research Foundation (to J.R.W.). We thank Doriane LeBourse for assistance with T-DNA mutant screening and subcloning of *At4g19010* cDNA.

Author Contributions

A.B., J.R.W., R.E.C., and G.J.B. designed and performed the research, analyzed the data, and wrote the article. A.F., Y.W., and C.E. performed the research and analyzed the data. S.A.M., E.B.C., C.C., and N.D. analyzed the data.

References

Achnine, L., Blancaflor, E.B., Rasmussen, S., and Dixon, R.A. (2004). Colocalization of L-phenylalanine ammonia-lyase and cinnamate 4-hydroxylase for metabolic channeling in phenylpropanoid biosynthesis. Plant Cell 16: 3098–3109.

Alonso, J.M., et al. (2003). Genome-wide insertional mutagenesis of *Arabidopsis thaliana*. Science 301: 653–657.

Avelange-Macherel, M.-H., and Joyard, J. (1998). Cloning and functional expression of AtCOQ3, the Arabidopsis homologue of the yeast COQ3 gene, encoding a methyltransferase from plant mitochondria involved in ubiquinone biosynthesis. Plant J. 14: 203–213.

Block, A., Fristedt, R., Rogers, S., Kumar, J., Barnes, B., Barnes, J., Elowsky, C.G., Wamboldt, Y., Mackenzie, S.A., Redding, K., Merchant, S.S., and Basset, G.J. (2013). Functional modeling identifies paralogous solanesyl-diphosphate synthases that assemble the side chain of plastoquinone-9 in plastids. J. Biol. Chem. 288: 27594–27606.

Block, A., Guo, M., Li, G., Elowsky, C., Clemente, T.E., and Alfano, J.R. (2010). The *Pseudomonas syringae* type III effector HopG1 targets mitochondria, alters plant development and suppresses plant innate immunity. Cell. Microbiol. 12: 318–330.

Bradford, M.M. (1976). A rapid and sensitive method for the quantitation of microgram quantities of protein utilizing the principle of protein-dye binding. Anal. Biochem. 72: 248–254.

Bussell, J.D., Reichelt, M., Wiszniewski, A.A., Gershenzon, J., and Smith, S.M. (2014). Peroxisomal ATP-binding cassette transporter COMATOSE and the multifunctional protein abnormal INFLORESCENCE MERISTEM are required for the production of benzoylated metabolites in Arabidopsis seeds. Plant Physiol. 164: 48–54.

Cardazzo, B., Hamel, P., Sakamoto, W., Wintz, H., and Dujardin, G. (1998). Isolation of an *Arabidopsis thaliana* cDNA by complementation of a yeast abc1 deletion mutant deficient in complex III respiratory activity. Gene 221: 117–125.

Clarke, C.F. (2000). New advances in coenzyme Q biosynthesis. Protoplasma 213: 134–147.

Clough, S.J., and Bent, A.F. (1998). Floral dip: a simplified method for *Agrobacterium*-mediated transformation of *Arabidopsis thaliana*. Plant J. 16: 735–743.

Colquhoun, T.A., Marciniak, D.M., Wedde, A.E., Kim, J.Y., Schwieterman, M.L., Levin, L.A., Van Moerkercke, A., Schuurink, R.C., and Clark, D.G. (2012). A peroxisomally localized acyl-activating enzyme is required for volatile benzenoid formation in a *Petunia*3*hybrida* cv. 'Mitchell Diploid' flower. J. Exp. Bot. 63: 4821–4833.

Costa, M.A., et al. (2005). Characterization in vitro and in vivo of the putative multigene 4-coumarate:CoA ligase network in *Arabidopsis*: syringyl lignin and sinapate/sinapyl alcohol derivative formation. Phytochemistry 66: 2072–2091.

Dawson, R.M.C., Elliot, D.C., Elliot, W.H., and Jones, K.M. (1986). Data for Biochemical Research. (New York: Oxford University Press).

DellaPenna, D., and Pogson, B.J. (2006). Vitamin synthesis in plants: tocopherols and carotenoids. Annu. Rev. Plant Biol. 57: 711–738.

De Marcos Lousa, C., van Roermund, C.W., Postis, V.L., Dietrich, D., Kerr, I.D., Wanders, R.J., Baldwin, S.A., Baker, A., and Theodoulou, F.L. (2013). Intrinsic acyl-CoA thioesterase activity of a peroxisomal ATP binding cassette transporter is required for transport and metabolism of fatty acids. Proc. Natl. Acad. Sci. USA 110: 1279–1284.

Ducluzeau, A.-L., Wamboldt, Y., Elowsky, C.G., Mackenzie, S.A., Schuurink, R.C., and Basset, G.J.C. (2012). Gene network reconstruction identifies the authentic trans-prenyl diphosphate synthase that makes the solanesyl moiety of ubiquinone-9 in Arabidopsis. Plant J. 69: 366–375.

Egland, P.G., and Harwood, C.S. (2000). HbaR, a 4-hydroxybenzoate sensor and FNR-CRP superfamily member, regulates anaerobic 4-hydroxybenzoate degradation by *Rhodopseudomonas palustris*. J. Bacteriol. 182: 100–106.

Ehlting, J., Büttner, D., Wang, Q., Douglas, C.J., Somssich, I.E., and Kombrink, E. (1999). Three 4-coumarate:coenzyme A ligases in *Arabidopsis thaliana* represent two evolutionarily divergent classes in angiosperms. Plant J. 19: 9–20.

Footitt, S., Slocombe, S.P., Larner, V., Kurup, S.,Wu, Y., Larson, T., Graham, I., Baker, A., and Holdsworth, M. (2002). Control of germination and lipid mobilization by COMATOSE, the Arabidopsis homologue of human ALDP. EMBO J. 21: 2912–2922.

Forner, J., and Binder, S. (2007). The red fluorescent protein eqFP611: application in subcellular localization studies in higher plants. BMC Plant Biol. 7: 28.

Gaid, M.M., Sircar, D., Müller, A., Beuerle, T., Liu, B., Ernst, L., Hänsch, R., and Beerhues, L. (2012). Cinnamate:CoA ligase initiates the biosynthesis of a benzoate-derived xanthone phytoalexin in *Hypericum calycinum* cell cultures. Plant Physiol. 160: 1267–1280.

Hajdukiewicz, P., Svab, Z., and Maliga, P. (1994). The small, versatile pPZP family of Agrobacterium binary vectors for plant transformation. Plant Mol. Biol. 25: 989–994.

Hamberger, B., and Hahlbrock, K. (2004). The 4-coumarate:CoA ligase gene family in *Arabidopsis thaliana* comprises one rare, sinapate-activating and three commonly occurring isoenzymes. Proc. Natl. Acad. Sci. USA 101: 2209–2214.

Karimi, M., Inzé, D., and Depicker, A. (2002). GATEWAY vectors for Agrobacterium-mediated plant transformation. Trends Plant Sci. 7: 193–195.

Kawamukai, M. (2009). Biosynthesis and bioproduction of coenzyme Q10 by yeasts and other organisms. Biotechnol. Appl. Biochem. 53: 217–226.

Kienow, L., Schneider, K., Bartsch, M., Stuible, H.P., Weng, H., Miersch, O., Wasternack, C., and Kombrink, E. (2008). Jasmonates meet fatty acids: functional analysis of a new acyl-coenzyme A synthetase family from *Arabidopsis thaliana*. J. Exp. Bot. 59: 403–419.

Klempien, A., et al. (2012). Contribution of CoA ligases to benzenoid biosynthesis in petunia flowers. Plant Cell 24: 2015–2030.

Kliebenstein, D.J., D'Auria, J.C., Behere, A.S., Kim, J.H., Gunderson, K.L., Breen, J.N., Lee, G., Gershenzon, J., Last, R.L., and Jander, G. (2007). Characterization of seed-specific benzoyloxyglucosinolate mutations in *Arabidopsis thaliana*. Plant J. 51: 1062–1076.

Koo, A.J.K., Chung, H.S., Kobayashi, Y., and Howe, G.A. (2006). Identification of a peroxisomal acyl-activating enzyme involved in the biosynthesis of jasmonic acid in *Arabidopsis*. J. Biol. Chem. 281: 33511–33520.

Law, A.H., Threlfall, D.R., and Whistance, G.R. (1971). Isoprenoid phenol and quinone precursors of ubiquinones and dihydroubiquinones [Ubiquinones (H2)] in fungi. Biochem. J. 123: 331–339.

Lee, D., Meyer, K., Chapple, C., and Douglas, C.J. (1997). Antisense suppression of 4-coumarate:coenzyme A ligase activity in *Arabidopsis* leads to altered lignin subunit composition. Plant Cell 9: 1985–1998.

Lee, S., Kaminaga, Y., Cooper, B., Pichersky, E., Dudareva, N., and Chapple, C. (2012). Benzoylation and sinapoylation of glucosinolate R-groups in *Arabidopsis*. Plant J. 72: 411–422.

Löscher, R., and Heide, L. (1994). Biosynthesis of *p*-hydroxybenzoate from *p*-coumarate and *p*-coumaroyl-CoA in cell-free extracts of *Lithospermum erythrorhizon* cell cultures. Plant Physiol. 106: 271–279.

Marbois, B., Xie, L.X., Choi, S., Hirano, K., Hyman, K., and Clarke, C.F. (2010). para-Aminobenzoic acid is a precursor in coenzyme Q6 biosynthesis in *Saccharomyces cerevisiae*. J. Biol. Chem. 285: 27827–27838.

Nichols, B.P., and Green, J.M. (1992). Cloning and sequencing of *Escherichia coli* ubiC and purification of chorismate lyase. J. Bacteriol. 174: 5309–5316.

Nowicka, B., and Kruk, J. (2010). Occurrence, biosynthesis and function of isoprenoid quinones. Biochim. Biophys. Acta 1797: 1587–1605.

Obayashi, T., Hayashi, S., Saeki, M., Ohta, H., and Kinoshita, K. (2009). ATTED-II provides coexpressed gene networks for *Arabidopsis*. Nucleic Acids Res. 37: D987–D991.

Okada, K., Ohara, K., Yazaki, K., Nozaki, K., Uchida, N., Kawamukai, M., Nojiri, H., and Yamane, H. (2004). The AtPPT1 gene encoding 4-hydroxybenzoate polyprenyl diphosphate transferase in ubiquinone biosynthesis is required for embryo development in *Arabidopsis thaliana*. Plant Mol. Biol. 55: 567–577.

Olson, R.E., Bentley, R., Aiyar, A.S., Dialameh, G.H., Gold, P.H., Ramsey, V.G., and Springer, C.M. (1963). Benzoate derivatives as intermediates in the biosynthesis of coenzyme Q in the rat. J. Biol. Chem. 238: 3146–3148.

Pierrel, F., Hamelin, O., Douki, T., Kieffer-Jaquinod, S., Mühlenhoff, U., Ozeir, M., Lill, R., and Fontecave, M. (2010). Involvement of mitochondrial ferredoxin and para-aminobenzoic acid in yeast coenzyme Q biosynthesis. Chem. Biol. 17: 449–459.

Pribat, A., et al. (2010). Nonflowering plants possess a unique folatedependent phenylalanine hydroxylase that is localized in chloroplasts. Plant Cell 22: 3410–3422.

Qualley, A.V., Widhalm, J.R., Adebesin, F., Kish, C.M., and Dudareva, N. (2012). Completion of the core b-oxidative pathway of benzoic acid biosynthesis in plants. Proc. Natl. Acad. Sci. USA 109: 16383–16388.

Quinlivan, E.P., Roje, S., Basset, G., Shachar-Hill, Y., Gregory, J.F., III., and Hanson, A.D. (2003). The folate precursor p-aminobenzoate is reversibly converted to its glucose ester in the plant cytosol. J. Biol. Chem. 278: 20731–20737.

Pfaff, C., Glindemann, N., Gruber, J., Frentzen, M., and Sadre, R. (2014). Chorismate pyruvate-lyase and 4-hydroxy-3-solanesylbenzoate decarboxylase are required for plastoquinone biosynthesis in the cyanobacterium *Synechocystis* sp. PCC6803. J. Biol. Chem. 289: 2675–2686.

Reumann, S. (2013). Biosynthesis of vitamin k1 (phylloquinone) by plant peroxisomes and its integration into signaling molecule synthesis pathways. Subcell. Biochem. 69: 213–229.

Richmond, T.A., and Bleecker, A.B. (1999). A defect in beta-oxidation causes abnormal inflorescence development in Arabidopsis. Plant Cell 11: 1911–1924.

Robinson, S.J., et al. (2009). An archived activation tagged population of *Arabidopsis thaliana* to facilitate forward genetics approaches. BMC Plant Biol. 9: 101.

Schilmiller, A.L., Stout, J., Weng, J.K., Humphreys, J., Ruegger, M.O., and Chapple, C. (2009). Mutations in the cinnamate 4-hydroxylase gene impact metabolism, growth and development in Arabidopsis. Plant J. 60: 771–782.

Shockey, J., and Browse, J. (2011). Genome-level and biochemical diversity of the acyl-activating enzyme superfamily in plants. Plant J. 66: 143–160.

Van Moerkercke, A., Schauvinhold, I., Pichersky, E., Haring, M.A., and Schuurink, R.C. (2009). A plant thiolase involved in benzoic acid biosynthesis and volatile benzenoid production. Plant J. 60: 292–302.

Widhalm, J.R., Ducluzeau, A.-L., Buller, N.E., Elowsky, C.G., Olsen, L.J., and Basset, G.J.C. (2012). Phylloquinone (vitamin K(1)) biosynthesis in plants: two peroxisomal thioesterases of lactobacillales origin hydrolyze 1,4-dihydroxy-2-naphthoyl-coa. Plant J. 71: 205–215.

Zolman, B.K., Silva, I.D., and Bartel, B. (2001). The Arabidopsis pxa1 mutant is defective in an ATP-binding cassette transporter-like protein required for peroxisomal fatty acid b-oxidation. Plant Physiol. 127: 1266–1278.

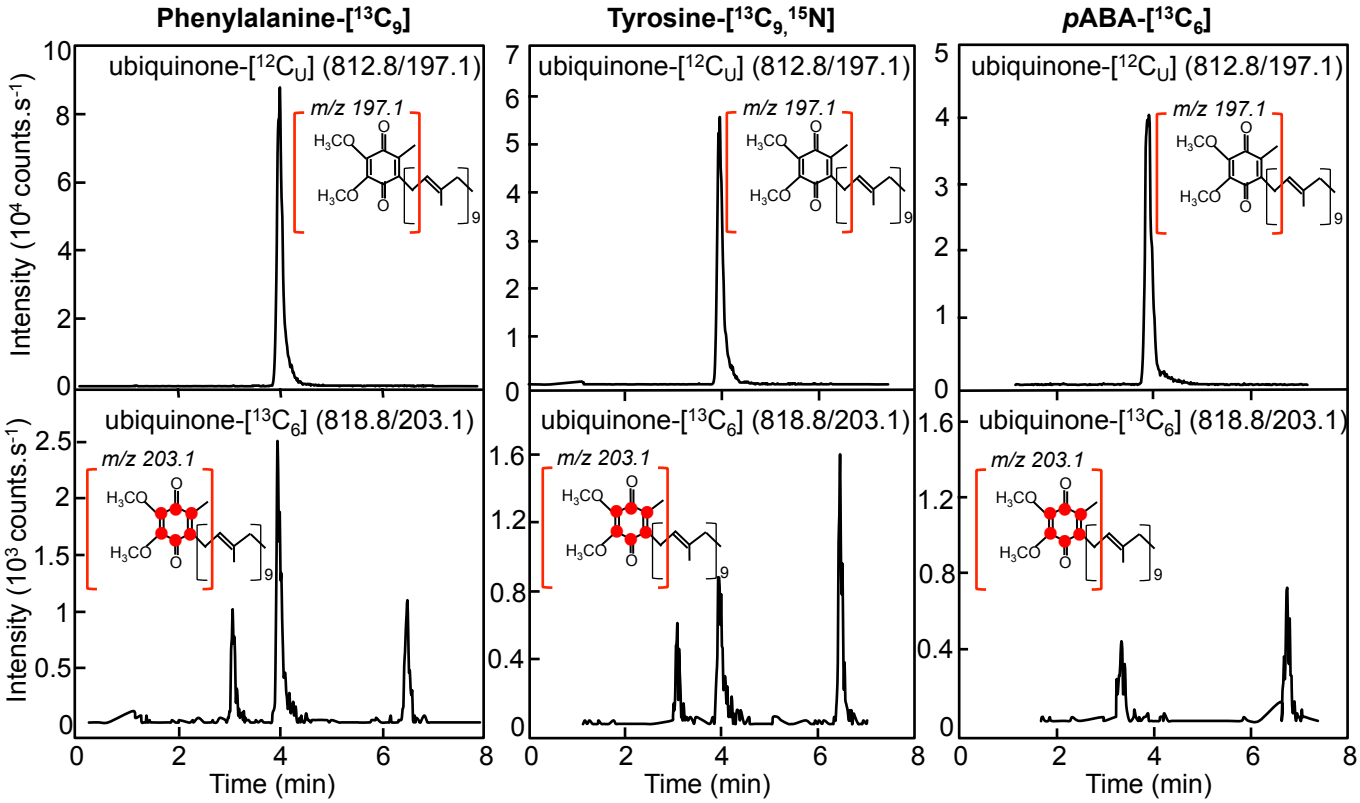

Supplemental Figure 1. Extracted counts of ion pairs for multiple reaction monitorings of ubiquinone isotopes. Axenically grown Arabidopsis were fed for 3h with 250 µM doses of phenylalanine-[$^{13}C_9$] (left panels), tyrosine-[$^{13}C_9$;^{15}N] (center panels) or *p*ABA-[$^{13}C_6$] (right panels). Red dots indicate the positions of the ^{13}C isotope.

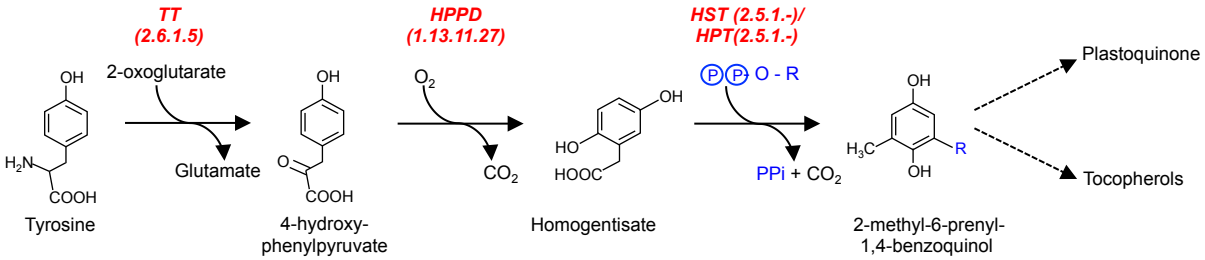

Supplemental Figure 2. Formation of the ring of plastid prenyl benzoquinones from tyrosine**.** R is phytyl (C_{20}) in the biosynthetic pathway of tocopherols, and solanesyl (C_{45}) in that of plastoquinone. HPPD, 4-hydroxyphenylpyruvate dioxygenase; HPT, homogentisate phytyl transferase; HST, homogentisate solanesyl transferase; TT, tyrosine transaminase

Supplemental Table 1. CoA ligase activity in Arabidopsis extracts

	nmoles.mg^{-1}.h^{-1}			
	p-coumarate	*t*-cinnamate	Ferulate	Caffeate
Wild type	49 ± 18	12 ± 5	31 ± 8	48 ± 11
at4g19010	54 ± 29	14 ± 9	44 ± 18	50 ± 13

Arabidopsis leaf extracts (18-36 μg) were assayed with 2.5 mM ATP, 0.5 mM CoA and 100 μM of various hydroxycinnamate derivatives for 30-60 min at 30°C. The formation of the corresponding CoA thioesters was monitored spectrophotometrically as described in the Methods. Data are means of three replicates ± S.E. Wild-type and *at4g19010* knockout (SALK_043310) values are not significantly different as determined by Fisher's test from an analysis of variance ($p>0.3$).

Block et al. Plant Cell (2014) 10.1105/tpc.114.125807

	Locus	Alias	Function	MR(all)	MR(tissue)	MR(abiotic)	MR(biotic)	MR(hormone	MR(light)
0	At4g19010	ligase	AMP-dependent synthetase and ligase family protein	0	0	0	0	0	0
1	At1g66660	Protein with	Protein with RING/U-box and TRAF-like domains	9.4	661.4	38.2	781.6	851	7998.1
2	At5g50960	NBP35	nucleotide binding protein 35	12.2	407.5	235.6	336.4	928.2	1961.5
3	At3g51790	TG1	transmembrane protein G1P-related 1	12.5	315.7	114.3	1462.7	173.5	907.8
4	At4g37120	SMP2	Pre-mRNA splicing Prp18-interacting factor	27.1	156.1	177.2	17.1	300	5800.6
5	At3g03950	ECT1	evolutionarily conserved C-terminal region 1	29.9	1301.4	7	1395.3	2066.2	3477.9
6	At1g17130	DUF572	Family of unknown function (DUF572)	30.7	2136.2	82.2	1496.6	206.1	5428.6
7	At4g39160	Homeodoma	Homeodomain-like superfamily protein	33.5	270	109.9	923.2	1958.6	5728.5
8	At1g04860	UBP2	ubiquitin-specific protease 2	36.3	1564.5	116.1	2861.7	7808.8	2999.1
9	At1g74250	N-terminal	DNAJ heat shock N-terminal domain-containing protein	36.3	291.6	146.3	3141.5	284.5	12232.5
10	At1g48970	NagB	NagB/RpiA/CoA transferase-like superfamily protein	45.9	993.3	178.3	1182.4	1036.2	1454.7
11	At5g55200	MGE1	Co-chaperone GrpE family protein	48.2	248.3	205.8	177	3598.8	755.2
12	At2g04740	ankyrin repe	ankyrin repeat family protein	49.8	364.3	24.5	2869.9	12845.8	396.6
13	At2g34630	SPS3	Solanesyl diphosphate synthase 3	57.4	222.6	289.1	703.1	262.7	5792.2
14	At2g30640	transposable	transposable element gene	58.6	2857.4	145.2	2184.5	2651.5	5153.8
15	At5g26860	LON_ARA_AF	lon protease 1	78.4	961	137.8	1946.3	2068	614.8
16	At3g22980	G/III/V	Ribosomal protein S5/Elongation factor G/III/V family protein	81.3	397.9	390.5	137.4	1125.1	2525.5
17	At4g09680	CTC1	conserved telomere maintenance component 1	100.4	109.4	457.1	5332.4	1514.6	7498.4
18	At3g01800	Ribosome re	Ribosome recycling factor	101.7	422	303	2173.2	2269.2	1554.2
19	At3g26400	EIF4B1	eukaryotic translation initiation factor 4B1	102.2	1943.2	15.3	941.8	888.2	4311.4
20	At1g18480	SLP2	Calcineurin-like metallo-phosphoesterase superfamily protein	113.1	359.3	407.2	808.7	1613.2	4221.3
21	246147_s_at		At5g19990;At5g20000	113.4	3147.3	131.7	277.3	4986.7	1258.1
22	At5g05210	Surfeit locus	Surfeit locus protein 6	113.7	1751	445.1	1232.7	1517.6	7367.2
23	At1g09810	ECT11	evolutionarily conserved C-terminal region 11	115.1	1626.6	353.3	3656.9	3839.6	9784.7
24	At1g16650	transferase	S-adenosyl-L-methionine-dependent methyltransferases superfamily protein	115.4	953.3	1052.4	2160.2	3139.1	3968
25	At2g20330	Transducin/W	Transducin/WD40 repeat-like superfamily protein	116.9	571.6	258.8	3087.4	984.5	2148.7
26	At3g59280	TXR1	Protein Transporter, Pam16	118.4	836.8	470.3	930.8	5174.8	4365.8
27	At4g11140	CRF1	cytokinin response factor 1	120.7	661.5	1008.2	7011.2	16575.2	8040.4
28	At1g04945	HIT-type Zinc	HIT-type Zinc finger family protein	120.8	2372	107.1	2786	2561.9	759
29	At1g20100			127.9	24.7	733.5	2755.8	3027.2	17063.2
30	At1g13870	DRL1	calmodulin binding;purine nucleotide binding	128	695.9	259.2	1607.2	2656.8	6583.6
31	At1g31600	TRM9	RNA-binding (RRM/RBD/RNP motifs) family protein	132	23.2	1143.5	6063.6	298.3	8637.4
32	At3g08950	HCC1	electron transport SCO1/SenC family protein	144.8	1640.5	333.8	533	1609.7	5912.2
33	At3g47120	RRM	RNA recognition motif (RRM)-containing protein	145.4	1381.8	554.5	395.7	2658.2	10972.7
34	At5g40930	TOM20-4	translocase of outer membrane 20-4	146.7	9821.9	511.4	737.9	2327.5	3670.4
35	At2g02880	mucin	mucin-related	151.2	5790.6	60.6	3032.9	6549.8	8606.6
36	At1g43860	transcription	sequence-specific DNA binding transcription factors	152.7	7024.6	185.4	1711.9	1418.7	1389.4
37	At1g74750	PPR	Pentatricopeptide repeat (PPR) superfamily protein	152.8	1275	1012.8	1909.8	1990.8	802.8
38	At1g51710	UBP6	ubiquitin-specific protease 6	158.2	2253.8	99	626.3	3896.4	1211.6
39	At2g44520	COX10	cytochrome c oxidase 10	165	2628.8	37.5	665.5	856.9	1331.3
40	At5g37570	PPR-like	Pentatricopeptide repeat (PPR-like) superfamily protein	169.3	977.1	447.8	6100.4	1719.9	7024.2
41	At1g77570	DNA-binding	Winged helix-turn-helix transcription repressor DNA-binding	171.2	2146.5	185.5	3103.1	12778.6	651.2
42	At1g04930	glycoprotein	hydroxyproline-rich glycoprotein family protein	172.5	152.9	458.6	5821.7	2249.9	15561.5
43	At4g16440	ferredoxin hy	ferredoxin hydrogenases	172.9	1353.2	344.1	1617.2	949	5285.3
44	At5g20910	RING	RING/U-box superfamily protein	174.9	7369.1	454.6	65.1	3838.5	791.1
45	At1g76810	eIF-2	eukaryotic translation initiation factor 2 (eIF-2) family protein	175.6	2426.4	82.3	1175.4	1849.2	3504.4
46	At2g35510	SRO1	similar to RCD one 1	176.4	99.1	400.5	2591.3	3297.4	3954.7
47	At3g21140	oxidase	Pyridoxamine 5'-phosphate oxidase family protein	177.6	3059.3	734.4	634.3	320.5	5595.9
48	At4g37090			177.9	3111.5	504.6	3087.2	4359.5	7268.6
49	At5g03030	DnaJ-domain	Chaperone DnaJ-domain superfamily protein	179.2	1484.5	68	3390.4	3608	1857.2
50	At3g10370	SDP6	FAD-dependent oxidoreductase family protein	182.9	1135.1	230.7	2007.9	3153.6	7965
51	At3g55620	emb1624	Translation initiation factor IF6	183.8	814.8	1036.9	316.2	1252.2	1580.7
52	At4g11160	GTP-binding	Translation initiation factor 2, small GTP-binding protein	187.6	1358.9	582.9	1733.5	818.1	3845
53	At5g30490			190.1	3824	105.4	1839.7	3235.7	7634.9
54	At5g59980	Polymerase/I	Polymerase/histidinol phosphatase-like	190.3	4540.2	186.7	7454.7	495.5	578.5
55	At2g24500	FZF	Zinc finger protein 622	196.2	9505.6	106.4	675.4	372.9	1070.2
56	At4g08460	DUF1644	Protein of unknown function (DUF1644)	196.7	2994.5	312.8	67.3	976.5	13517.7
57	At5g64400			198.2	647.5	305.1	1419.6	5109.2	7854.2
58	At2g03820	NMD3	nonsense-mediated mRNA decay NMD3 family protein	200.9	2656.6	71	1778.8	4198.6	624.2
59	At5g51130	transferase	S-adenosyl-L-methionine-dependent methyltransferases superfamily protein	201.2	2029	15	3479	1152.6	1294.3
60	At4g20090	EMB1025	Pentatricopeptide repeat (PPR) superfamily protein	208.2	2553.1	23.8	9906.7	1265.2	781.6
61	At1g61640	kinase	Protein kinase superfamily protein	208.9	2577.4	141.5	4231.8	222.4	1949.5
62	At3g18100	MYB4R1	myb domain protein 4r1	210	2455.3	116.9	2842.2	3474.3	10735.1
63	At3g12340	isomerase	FKBP-like peptidyl-prolyl cis-trans isomerase family protein	210.5	3821.2	44.8	2031.3	1345.8	7314
64	At1g16540	SIR3	molybdenum cofactor sulfurase (LOS5) (ABA3)	210.6	2082.4	315.7	40.9	478.2	4637.5
65	At5g13070	MSF1-like	MSF1-like family protein	211.1	1278.5	836.5	1199.6	2187.7	2163.5
66	At3g12640	RNA binding	RNA binding (RRM/RBD/RNP motifs) family protein	218.6	6462.3	26.9	2229	3768.4	3675.5
67	At1g55820	DUF1296	Kinase-related protein of unknown function (DUF1296)	218.8	5654.1	262.4	920.5	3096.3	12419.5
68	At5g06110	DnaJ domain	DnaJ domain ;Myb-like DNA-binding domain	226.9	7706.2	115.5	1362.2	4846.5	2435.7
69	At2g16860	GCIP-interact	GCIP-interacting family protein	227.4	725.5	167.5	2835.5	1526.1	8188.8
70	At5g25060	RRM	RNA recognition motif (RRM)-containing protein	231.5	113.8	111.7	739.2	1820.2	4451.6
71	At2g19270			236.3	8942.6	231.7	973.6	1484.2	5492.7
72	At5g27540	MIRO1	MIRO-related GTP-ase 1	237.7	4675.8	356	435.2	41.5	2902.3
73	At1g14300	ARM repeat	ARM repeat superfamily protein	238.7	1139.1	64.8	1049.7	3277.5	3176.3
74	At4g36580	ATPase	AAA-type ATPase family protein	240.1	2086.9	266.3	4406.7	8820.3	1363.5
75	At1g10270	GRP23	glutamine-rich protein 23	241.4	6603.1	95	3908.1	1595.9	1025
76	At1g60620	RPAC43	RNA polymerase I subunit 43	244.2	1653.3	188.6	1658.6	1201.9	5764.8
77	At3g44680	HDA9	histone deacetylase 9	247.4	3170.3	195.2	2058	366.1	3159.6
78	At1g55870	PARN	Polynucleotidyl transferase, ribonuclease H-like superfamily protein	251.8	3645.5	30.9	8036.9	7736.2	7007.9

	Locus	Alias	Function	MR(all)	MR(tissue)	MR(abiotic)	MR(biotic)	MR(hormone	MR(light)
79	At1g15860	DUF298	Domain of unknown function (DUF298)	253.4	9578.3	31.8	648.9	5261.7	706.5
80	At1g55080	MED9		254.5	1138.8	1497.7	312.9	1516.4	9541.1
81	At1g55170			256.3	881.9	2831.4	2957.1	1187.2	5465.9
82	At5g51700	RPR2	protein binding;zinc ion binding	267.5	4109.5	2272.2	1542.5	493.3	4115.1
83	At3g21175	ZML1	ZIM-like 1	270	2575.4	849.4	1777.7	928.8	1624.6
84	At2g14850			270.3	1788.8	379.2	1929	3766.7	5783.6
85	At5g52380	VASCULAR-RI	VASCULAR-RELATED NAC-DOMAIN 6	274.9	6249.9	391	2810	664.8	3117.3
86	At2g35736			275.9	2530.8	824.4	1169.5	16280.4	6482
87	At5g23520	smr	smr (Small MutS Related) domain-containing protein	276.2	1601.4	142.8	2737.4	3966.2	14797
88	At3g01540	DRH1	DEAD box RNA helicase 1	277.9	3802.2	585.4	830.4	243.9	9546.2
89	At4g21090	MFDX2	MITOCHONDRIAL FERREDOXIN 2	278	4560.3	195.3	1613.6	432.7	2011.5
90	At3g54170	FIP37	FKBP12 interacting protein 37	282.6	3022.2	1.4	5800.2	4637.8	7396.2
91	At5g22840	kinase	Protein kinase superfamily protein	285.9	4496.6	152.4	4349.7	4562	2132.9
92	At5g63120	hydrolase	P-loop containing nucleoside triphosphate hydrolases superfamily protein	291.8	477.9	1356.1	1966.2	28.6	10933.6
93	At1g51380	helicase	DEA(D/H)-box RNA helicase family protein	292.2	2950.6	230.1	4351.2	5054.4	780.6
94	At5g12290	DGS1	dgd1 suppressor 1	292.4	2259.8	1342.2	2527.3	932.4	1707.3
95	At3g20430			296.2	4373.9	420.9	8649.9	1985.3	4726.9
96	At3g15180	ARM repeat	ARM repeat superfamily protein	303.9	2122	1262.3	501.4	2774	713.8
97	At4g16845	VRN2	VEFS-Box of polycomb protein	304.6	2359.6	141.8	530.1	195.2	9699.5
98	At3g49320	hydrolase	Metal-dependent protein hydrolase	307.9	3090.2	189.2	4335.8	4553.1	3743.8
99	At1g69250	NTF2	Nuclear transport factor 2 (NTF2) family protein with RNA binding (RRM-RBD-RNP motifs	309.8	3533	652.9	2049.9	3058.1	1295.3
100	At5g18400	inhibitor	Cytokine-induced anti-apoptosis inhibitor 1, Fe-S biogenesis	320	1105.3	283.8	4389.8	708.2	2436.4
101	At1g50400	Eukaryotic pc	Eukaryotic porin family protein	323.3	845	92.9	9052.9	15114.3	1354.8
102	At1g28210	ATJ1	DNAJ heat shock family protein	323.9	1049.7	48.2	1524.8	2410.3	14844.8
103	At1g33390	FAS4	RNA helicase family protein	324.1	3180.5	843.5	3303.5	2301	9787.5
104	At4g04180	hydrolase	P-loop containing nucleoside triphosphate hydrolases superfamily protein	326.4	4494.7	198.1	4979.9	8149.6	10522.6
105	At2g45690	SSE1	shrunken seed protein (SSE1)	332	224.4	2823.5	3056.3	3763.5	13937.9
106	At1g75670	RNA polymer	DNA-directed RNA polymerases	332.2	5920.8	199.2	3289	3991.3	502.6
107	At3g02320	transferase	N2,N2-dimethylguanosine tRNA methyltransferase	333.5	5625.1	491.4	2235.6	1490.3	5848.5
108	At5g16780	MDF	SART-1 family	340.1	2824.3	182.4	1385.9	611.9	5786.1
109	At2g44200	splicing	CBF1-interacting co-repressor CIR, N-terminal;Pre-mRNA splicing factor	344.4	1290.9	308.1	2070.5	1036.5	5607.3
110	At5g44780			344.8	3608.1	433.8	4601.4	7308.3	4546.5
111	At3g17740			346.6	1286	123.6	3333.6	3858.9	9237.1
112	At1g16210			347.5	3853.3	649.9	264.7	586.4	5585.6
113	At4g26800	PPR	Pentatricopeptide repeat (PPR) superfamily protein	347.5	2277.3	170.9	8498.3	1821.3	4597.2
114	At1g14060	GCK	GCK domain-containing protein	350.5	1430.5	840.5	3176.4	9087.6	970.6
115	At2g23080	CKA3	Protein kinase superfamily protein	350.7	2720.5	5477.5	1830	887.2	2953.3
116	At2g35720	OWL1	DNAJ heat shock N-terminal domain-containing protein	354.1	288.9	1162.4	2685.2	2814.6	1078.3
117	At5g63010	Transducin/V	Transducin/WD40 repeat-like superfamily protein	355	5621.8	510.3	176.1	1989	4271.6
118	At5g42150	transferase	Glutathione S-transferase family protein	355.1	2694	442.1	2415.5	2147.5	4180.1
119	At3g15080	H-like	Polynucleotidyl transferase, ribonuclease H-like superfamily protein	357.1	9789.9	164.6	2802.1	1317.3	1447.4
120	At5g43130	TAF4B	TBP-associated factor 4	359.4	784.1	791.5	726.7	1329.3	4742.1
121	At2g03800	GEK1	D-aminoacyl-tRNA deacylases	360.8	253.4	1499.8	1164	803.5	6719.9
122	At1g01910	hydrolase	P-loop containing nucleoside triphosphate hydrolases superfamily protein	362.2	9372	885.4	306.4	932.9	4612.4
123	At1g73350			363.7	1406.8	1504.2	3913.9	7157	18820.4
124	At3g15352	COX17	cytochrome c oxidase 17	364.7	3467.7	430.1	143.5	4000.1	1191.6
125	At5g09380	RPC4	RNA polymerase III RPC4	372.7	2737.2	411.4	2742.4	1899	16774.1
126	At3g56510	RNA-binding	RNA-binding (RRM/RBD/RNP motifs) family protein	373.7	6559.7	934.7	2466.9	781.7	1953.7
127	At1g78800	transferase	UDP-Glycosyltransferase superfamily protein	375.1	8904.7	1015	1625.4	1948.3	3806.1
128	At2g42280	DNA-binding	basic helix-loop-helix (bHLH) DNA-binding superfamily protein	377.3	1326.5	2627.5	1497.2	1873.4	11769.1
129	At1g64350	SEH1H	Transducin/WD40 repeat-like superfamily protein	378.8	1057.5	2339.6	1431.7	4034.9	44.5
130	256502_at		At1g36730;At1g36732	383.2	183.1	187.5	1670.8	1013.2	13281
131	At3g07370	CHIP	carboxyl terminus of HSC70-interacting protein	385	462.4	317.4	252	2308	13949.6
132	At5g58290	RPT3	regulatory particle triple-A ATPase 3	386.3	5199.2	1047.9	96.3	3418.4	577.3
133	At1g60850	RPAC42	DNA-directed RNA polymerase family protein	388.9	4544.3	220.6	3136	919.8	1815.7
134	At1g62260	MEF9	mitochondrial editing factor 9	391.1	2285.3	4000.2	14698.6	6591	9776.1
135	At1g53760			391.1	814.4	3054.3	242.7	1548.5	6933.3
136	At5g16930	ATPase	AAA-type ATPase family protein	391.7	3999.9	813.1	2271.5	1498.9	3687.9
137	At3g11220	ELO1	Paxneb protein-related	394.7	1557	1636.5	3623.8	2155.4	12778.1
138	250736_s_at		At1g01350;At5g06420	397.9	4940.7	426	2847.6	1837.7	7541.8
139	At5g26940	DPD1	Polynucleotidyl transferase, ribonuclease H-like superfamily protein	398.9	823.9	4297.7	1544.7	2152.3	2816.8
140	At2g31060	EMB2785	elongation factor family protein	406	539.6	1597	2962.1	1967	77.8
141	At5g22060	J2	DNAJ homologue 2	406.4	231.1	875.2	1844.1	1445.3	18919.1
142	At4g33650	DRP3A	dynamin-related protein 3A	408.7	80.9	3783.6	3255.9	2109	2329.2
143	At3g02010	PPR	Pentatricopeptide repeat (PPR) superfamily protein	409.5	2475.2	1314	10925.2	7396.4	9765.5
144	At5g46920	Intron matur	Intron maturase, type II family protein	411.1	4562.2	406.1	3238.5	3706.9	113.3
145	At4g15030			412.8	697.8	732.2	1475.4	590.8	14925.2
146	At1g03250			413.9	3715.8	2918.9	3060.4	5083.9	4084.6
147	At5g47080	CKB1	casein kinase II beta chain 1	414	377	774.6	1020	793.2	987.9
148	At2g36740	SWC2	sequence-specific DNA binding transcription factors;DNA binding;DNA binding	415.6	1180.2	335.1	3714.7	4959.7	7978.9
149	At5g62050	OXA1AT	homolog of yeast oxidase assembly 1 (OXA1)	420.3	1844.1	489.1	3090.1	2242.8	845.5
150	At4g03240	FH	frataxin homolog	422	3504.7	1920.5	4938.2	8553.4	4082.5
151	At3g06540	REP	Rab escort protein	426.5	2939.5	720.6	1222.7	1551.5	13477.8
152	At5g19490	Histone	Histone superfamily protein	429.8	372.1	2138.9	13157.1	17879	5518.1
153	At4g38380	MATE efflux	MATE efflux family protein	431	203.8	1317.1	10590.9	7677.6	8567.6
154	At1g68990	MGP3	male gametophyte defective 3	431.7	3569.5	90.3	3528.1	1150	2524.9
155	At1g12470	zinc ion bindi	zinc ion binding	431.9	6697.5	270.9	813.3	119.2	3031
156	At4g39520	GTP-binding	GTP-binding protein-related	435.7	1693.3	798.3	1242	1310	424.6
157	At1g02410	Cox11	cytochrome c oxidase assembly protein CtaG / Cox11 family	437	6596.9	997.3	8808.9	1392.6	7835.8

Block et al. Plant Cell (2014) 10.1105/tpc.114.125807

	Locus	Alias	Function	MR(all)	MR(tissue)	MR(abiotic)	MR(biotic)	MR(hormone	MR(light)
158	At1g52160	TRZ3	tRNAse Z3	439.9	3588.8	266.8	4287.2	2475.8	1265
159	At2g27100	SE	C2H2 zinc-finger protein SERRATE (SE)	440.8	7261.6	66.4	1946	533.6	1719.9
160	At1g22960	PPR	Pentatricopeptide repeat (PPR) superfamily protein	441.6	560.7	304	5539.9	4493.6	8873.8
161	At2g23470	RUS4	Protein of unknown function, DUF647	448.2	963	1326.7	17068.4	11393.7	10040.2
162	At2g37890	Mitochondria	Mitochondrial substrate carrier family protein	448.8	4395.2	178	4267.4	5212.4	601.2
163	261433_s_at		At1g07670;At1g07810	451.9	8130.5	958.7	506.8	1441.9	16933.5
164	At5g64730	Transducin/V	Transducin/WD40 repeat-like superfamily protein	454.2	4128	50	4085.9	1924	778.6
165	At3g43510	transposable	transposable element gene	454.3	1571.5	400.2	3304.1	953.8	3072.3
166	At4g03180			460.4	10994.4	221.1	3150.4	2537.6	3421.2
167	At4g03430	STA1	pre-mRNA splicing factor-related	460.5	4238.7	607.3	3105	1476.6	3167
168	At4g21140			461.5	4815.8	444.4	2861.1	2384.6	1432.8
169	At4g07990	DnaJ-domain	Chaperone DnaJ-domain superfamily protein	462.4	3084.9	711.6	1521.2	3006	6269.2
170	251951_s_at		At1g55710;At3g53630;At4g18692	462.7	3903.2	56.6	3456.2	7880.8	2462.7
171	252271_s_at		At3g49420;At5g01430	465.5	3183.3	970.3	252.4	816.7	2393.4
172	At1g26660	chaperonin	Prefoldin chaperone subunit family protein	468.2	981.8	2049.1	3163.3	4386	16151.1
173	At3g25545			468.7	8086.4	1106.4	1544.8	3106.3	1941.8
174	At4g13750	NOV	Histidine kinase-, DNA gyrase B-, and HSP90-like ATPase family protein	470.1	2170.7	279.2	4445.9	10154.2	12431.5
175	At1g24490	OxaA	OxaA/YidC-like membrane insertion protein	471.1	1580.8	243.6	5554.6	3029.1	3640.2
176	At2g45280	RAD51C	RAS associated with diabetes protein 51C	472.4	374.9	4753.8	3319.2	2930.6	10395.4
177	At5g11030	ALF4	aberrant lateral root formation 4	473.7	780.8	679.9	2806.5	17783.9	14511.5
178	At1g79730	ELF7	hydroxyproline-rich glycoprotein family protein	474.7	2597.2	198.8	1002.9	335.2	719.4
179	263422_s_at		At2g17190;At2g17200	477.1	2325.8	556.5	452.1	7844	1729.6
180	At5g53540	hydrolase	P-loop containing nucleoside triphosphate hydrolases superfamily protein	482.7	6706	24.6	4397.8	7087.4	7821.8
181	At5g12220	las1-like	las1-like family protein	482.8	6373.8	418.6	5501.5	4767.8	8480.7
182	At1g30240			482.9	3450.1	525.7	3897.9	3407.4	8321.2
183	262433_s_at		At1g47490;At1g47500	483.8	3499.4	1463.2	5410.6	1481.1	4794.1
184	At1g27760	SAT32	interferon-related developmental regulator family protein / IFRD protein family	492.8	2823.9	854.8	2144.6	2790.6	8013.5
185	At5g50780	ATPase	Histidine kinase-, DNA gyrase B-, and HSP90-like ATPase family protein	495.6	31.5	1666.5	1063.3	5396.3	16702.1
186	At4g30890	UBP24	ubiquitin-specific protease 24	495.9	4333.1	297.5	1939.3	597.4	1530.1
187	At1g29850	DNA-binding	double-stranded DNA-binding family protein	497	1493.7	6955	806.5	699.5	6981.9
188	At5g19400	SMG7	Telomerase activating protein Est1	501.1	166.8	788.7	1911.7	797.5	904.3
189	At1g66070	Translation ir	Translation initiation factor eIF3 subunit	501.9	10631.9	921.2	2567.6	1594.3	2793.3
190	At3g54380	SAC3	SAC3/GANP/Nin1/mts3/eIF-3 p25 family	503.8	744.4	3562.8	895.7	363.3	9087.8
191	At1g48120	hydrolase	hydrolases;protein serine/threonine phosphatases	506.6	1722.8	295.6	5641.3	2372.3	2561.5
192	At3g13200	EMB2769	Cwf15 / Cwc15 cell cycle control family protein	506.9	2259.8	963.1	479.7	2320.7	8642.2
193	At5g08310	Tetratricopep	Tetratricopeptide repeat (TPR)-like superfamily protein	509.9	1072.2	944	16079.1	9483.3	13699.8
194	At1g04810	proteasome	26S proteasome regulatory complex, non-ATPase subcomplex, Rpn2/Psmd1 subunit	512.5	9803.7	261.5	2214.7	5790.7	5186.6
195	At2g27600	VPS4	AAA-type ATPase family protein	512.7	2707.3	515.3	1707.4	422.6	438.7
196	At1g32130	IWS1	Transcription elongation factor (TFIIS) family protein	517	2236	130.6	684.5	2395.8	2126.3
197	261872_s_at		At1g11520;At4g21660	517.4	378.9	483.8	609.9	4587.7	12714.8
198	At2g40090	ATH9	ABC2 homolog 9	518.1	6354.6	5.9	2006.1	1719.7	1201
199	At2g47310	FCA gamma	flowering time control protein-related / FCA gamma-related	520.1	956.8	2379.5	7258.6	298.8	2453.2
200	At4g20330	Transcription	initiation factor TFIIE	Transcription	521.4	4753.3	412.1	405.1	3401.8
201	At4g02400	Utp	U3 ribonucleoprotein (Utp) family protein	522.6	8919.3	690.3	3735.3	1192.3	2926.1
202	At2g26590	RPN13	regulatory particle non-ATPase 13	528.3	7875.3	273.1	1002	872.5	1339
203	At3g03340	UNE6	LUC7 related protein	531.5	2961.9	1462	705.9	1596.8	2578.2
204	At1g08710	F-box	F-box family protein	532	357.8	1252.6	1618.4	2013.6	11178.6
205	At3g56990	EDA7	embryo sac development arrest 7	532.2	3309.9	488	4834.4	1753.9	2310.3
206	245437_at			538.6	2369.6	834.8	3718.1	5209.1	17300.9
207	At3g19630	SAM	Radical SAM superfamily protein	540.6	3126.9	937.2	2222.4	866.7	5858.7
208	At5g05520	OMP85	Outer membrane OMP85 family protein	543.5	3180.9	270.5	2751.6	6064.7	2607.6
209	At4g24200	TFIIS	Transcription elongation factor (TFIIS) family protein	545.7	480.5	1443.2	2362.1	6143.7	6089.4
210	At4g23540	ARM repeat	ARM repeat superfamily protein	546.5	2811.6	698.2	4266.9	1958.7	2245.3
211	At5g13970			547.2	4235.6	1193.2	5718.2	4890.3	5756.9
212	At3g04500	RNA-binding	RNA-binding (RRM/RBD/RNP motifs) family protein	549.5	1878.4	564.6	1655.1	4358.6	3382
213	At3g19760	EIF4A-III	eukaryotic initiation factor 4A-III	550	3882.3	1090.4	3862.4	2975.9	838.2
214	**At4g39850**	**PXA1**	**peroxisomal ABC transporter 1**	550	1111.3	928	385.3	578.2	9209
215	At1g31870			551.2	3450.8	262.5	2173.1	3618.3	2764.9
216	At5g04520	DUF455	Protein of unknown function DUF455	552.1	2046.4	951.3	656.8	767.1	15777.8
217	At1g31220	transferase	Formyl transferase	556.8	7347.8	28.7	11186.8	2071.5	11546.7
218	At5g07950			557.8	830.2	193	2319.1	2046.2	4554.7
219	260418_s_at		At1g66590;At1g69750	559.5	1765.3	313.5	413.8	4348.4	4610.4
220	At1g01940	isomerase	Cyclophilin-like peptidyl-prolyl cis-trans isomerase family protein	560.5	11262.6	388.7	1934.3	1453.2	3796.4
221	At4g19440	Tetratricopep	Tetratricopeptide repeat (TPR)-like superfamily protein	563	916.9	299	11625.1	4024.8	9832
222	At3g19670	PRP40B	pre-mRNA-processing protein 40B	563.5	46.8	506.8	1220.1	3829.6	7129.3
223	At2g47330	hydrolase	P-loop containing nucleoside triphosphate hydrolases superfamily protein	564.1	6524.6	142.2	1082.1	3798	3675.7
224	At1g72570	DNA-binding	Integrase-type DNA-binding superfamily protein	564.8	7904.7	15192.9	9711.3	4705.2	19222.9
225	At4g17830	M20/M25/M	Peptidase M20/M25/M40 family protein	565.9	5947.6	1988.1	1344.2	246.8	1338.8
226	At1g75510	Transcription	initiation factor IIF	Transcription	566.5	3978.9	1737	2650.4	1594.7
227	At3g19740	hydrolase	P-loop containing nucleoside triphosphate hydrolases superfamily protein	567.2	51.6	3327.5	4362.6	1475.7	6940.1
228	At1g42440			570.1	5252.1	550.5	3900.2	4031.9	898.1
229	At4g34910	hydrolase	P-loop containing nucleoside triphosphate hydrolases superfamily protein	571	5993.2	839.2	4496.6	2395.2	7905.4
230	At2g23890	nucleotidase	HAD-superfamily hydrolase, subfamily IG, 5'-nucleotidase	571.1	2926.2	56.1	3759.5	1878.7	3195.4
231	At5g19910	MED31	SOH1 family protein	571.8	4978.1	1316.7	4906.9	1586.2	1189
232	At5g17270	transferase	Protein prenylyltransferase superfamily protein	572.5	2780.1	263.1	5429.8	2059.8	3875.5
233	At3g05530	RPT5A	regulatory particle triple-A ATPase 5A	572.8	5190.4	2193.9	348.7	2722.5	15532.1
234	At5g40520			572.9	599.7	1136.8	4760.4	4377.8	7135.8
235	At5g56090	COX15	cytochrome c oxidase 15	578.2	3869.1	571.6	2065.4	853.4	5870.5
236	At1g13810	II-like	Restriction endonuclease, type II-like superfamily protein	581.7	2081.6	111.3	8767.6	6966	475.7

Block et al. Plant Cell (2014) 10.1105/tpc.114.125807

	Locus	Alias	Function	MR(all)	MR(tissue)	MR(abiotic)	MR(biotic)	MR(hormone	MR(light)
237	At5g46210	CUL4	cullin4	584	2997.6	263.5	4376.9	773	3172.7
238	At4g20060	EMB1895	ARM repeat superfamily protein	584.5	167.8	1310.5	3143.7	9512.5	17546.6
239	At1g01930	zinc finger	zinc finger protein-related	587.7	2124.7	149.8	7591.8	1517.6	7418.4
240	At3g11450	DnaJ domain	DnaJ domain ;Myb-like DNA-binding domain	590.8	877.4	1430.5	1654.1	6434.4	9236.2
241	249888_s_at		At5g22480;At5g37340	591.2	2842.6	958.3	1484.8	3385	4088.6
242	At1g80040			591.4	525.1	162.8	1610.6	7939.9	1933.6
243	At1g52730	Transducin/W	Transducin/WD40 repeat-like superfamily protein	591.8	3501.4	720.8	4068.8	3017.2	2281.3
244	**At4g01660**	**ATH10**	**ABC1-like**	592	4997	500.3	2283.3	3286.6	9018.1
245	At1g65020			592.2	11196.4	388	2082	3812.2	2710.9
246	At5g26110	kinase	Protein kinase superfamily protein	595	4208.9	1096	1494.3	934.4	2259.1
247	At4g02570	CUL1	cullin 1	601.7	4342.1	222.5	65.5	1142.6	454.9
248	At5g09420	TOC64-V	translocon at the outer membrane of chloroplasts 64-V	601.9	6350.8	135.7	4703.9	8242.8	1174.1
249	At3g17910	SURF1	Surfeit locus 1 cytochrome c oxidase biogenesis protein	602	2153.7	690.8	3340.6	2608.3	1682
250	At3g12140	EML1	Emsy N Terminus (ENT)/ plant Tudor-like domains-containing protein	603.1	1396.4	90	2748.3	2081.8	6210.3
251	At4g02220	C-terminal	zinc finger (MYND type) family protein / programmed cell death 2 C-terminal domain-cor	603.3	3066	564.5	3811.3	3011.2	12245.9
252	At3g51100			604.9	946.5	2459.1	906.1	12829.2	1649.8
253	At5g08510	PPR	Pentatricopeptide repeat (PPR) superfamily protein	605.5	104.3	2141.5	6429.6	10566.2	2211.7
254	At3g05360	RLP30	receptor like protein 30	607.8	2124.6	397.4	635	1757.2	3309.4
255	At3g03740	BPM4	BTB-POZ and MATH domain 4	608.3	2874.9	3172.4	846.7	395.6	2263.9
256	At1g66750	CDKD;2	CDK-activating kinase 4	609.8	5902.3	2496.6	9783.3	1016.7	9254.4
257	At2g47300	nuclease	ribonuclease Ps	611.8	997.5	1656.9	14909.9	7894.2	8802.6
258	At2g37250	PADK1	adenosine kinase	613.9	6961	603.4	1504.2	6749.8	1136.2
259	At5g15640	Mitochondria	Mitochondrial substrate carrier family protein	616.2	1431.5	2129.8	2213.6	207.8	2639.2
260	At1g06710	Tetratricopep	Tetratricopeptide repeat (TPR)-like superfamily protein	617.1	1540.5	758.1	14528.6	5508.7	4318.2
261	266932_s_at		At1g63250;At2g07750	617.5	7398.5	96.8	6975.1	8170.6	290
262	At3g47530	PPR	Pentatricopeptide repeat (PPR) superfamily protein	620.3	953.7	840.4	8555	7249.1	8571.9
263	At5g38890	OB-fold-like	Nucleic acid-binding, OB-fold-like protein	622.6	4757.1	516.4	2834	6170.5	1558.9
264	At4g27680	hydrolase	P-loop containing nucleoside triphosphate hydrolases superfamily protein	624.5	4487.2	1017.8	1019.7	6026.4	4254.7
265	At4g26600	transferase	S-adenosyl-L-methionine-dependent methyltransferases superfamily protein	625.5	5498.6	398.4	5598.1	1970.8	7343
266	At1g50140	hydrolase	P-loop containing nucleoside triphosphate hydrolases superfamily protein	627.7	475.8	1527.3	3134.1	660.3	8211.2
267	At1g55150	helicase	DEA(D/H)-box RNA helicase family protein	629.3	5568.6	30	4613.7	3078	5884.6
268	At5g27760	Hypoxia-resp	Hypoxia-responsive family protein	629.8	7101.4	1218	898.9	2809.9	899.6
269	At4g00090	Transducin/W	Transducin/WD40 repeat-like superfamily protein	630.7	12996.5	113.7	2622.5	2170.5	3841.1
270	At1g20300	PPR	Pentatricopeptide repeat (PPR) superfamily protein	630.8	7116.7	278.2	3787	1518.4	4343.3
271	At3g01610	emb1354	cell division cycle 48C	630.8	5275.7	322	4227.8	3310.8	2758
272	At5g42970	FUS8	Proteasome component (PCI) domain protein	631.4	7777.2	642.8	1746.6	347.7	2215.5
273	At5g14770	Tetratricopep	Tetratricopeptide repeat (TPR)-like superfamily protein	633.6	1497.7	281.7	8613	18589	6368.2
274	At4g28450	nucleotide bi	nucleotide binding;protein binding	637.4	6777	149.8	4318.6	4835.8	467.9
275	At5g53000	TAP46	2A phosphatase associated protein of 46 kD	637.7	5009.8	2198.7	2243	179.7	2433.1
276	At4g32660	AME3	Protein kinase superfamily protein	637.9	101.6	914.8	10237.1	871	6922.5
277	At3g11270	Mov34	Mov34/MPN/PAD-1 family protein	640	11005.8	953.4	913	3579	1219.1
278	At1g09100	RPT5B	26S proteasome AAA-ATPase subunit RPT5B	640.3	7401.7	1592.5	711.5	4201.1	2128.3
279	At1g63780	IMP4	Ribosomal RNA processing Brix domain protein	642.6	7087.3	184	4530.1	3813.2	1971.2
280	At1g13160	ARM repeat	ARM repeat superfamily protein	644.4	9377.6	596	3348.7	3862.7	3592.9
281	At4g03156	GTPase	small GTPase-related	648.5	1754	2253	9160.1	13123.6	15293.7
282	At1g71210	PPR	Pentatricopeptide repeat (PPR) superfamily protein	649.4	2512	377.5	4002.3	3526.8	2158
283	At5g11310	PPR	Pentatricopeptide repeat (PPR) superfamily protein	650.6	1598.3	147.1	4347.7	5860.9	4633.3
284	At3g15460	Ribosomal RN	Ribosomal RNA processing Brix domain protein	651.9	6264.4	897.9	5810.4	5430	1703.9
285	At1g80245	SBP	Spc97 / Spc98 family of spindle pole body (SBP) component	656	635.3	106.4	14451.8	6071.6	4535.2
286	At5g18420			658.8	6816.8	124.8	1812.1	4562.1	1643.7
287	At4g03260	Outer arm dy	Outer arm dynein light chain 1 protein	659.1	1110	711.5	6036.4	844.4	5283.9
288	At2g33730	hydrolase	P-loop containing nucleoside triphosphate hydrolases superfamily protein	660.3	6135.9	501.6	547	1660.3	1187.9
289	253890_s_at		At4g27585;At5g54100	661	5016.2	293.4	682.5	2436.3	1526
290	At5g15700	DNA	DNA/RNA polymerases superfamily protein	662.3	837	183.1	11418.2	14286.1	8988
291	At4g00170	VAMP	Plant VAMP (vesicle-associated membrane protein) family protein	662.5	1070.6	2710.1	2835.7	1553.2	1470.7
292	At2g39970	PXN	Mitochondrial substrate carrier family protein	664.4	394.9	7547.8	239.1	1995.1	13850.1
293	At5g49930	emb1441	zinc knuckle (CCHC-type) family protein	665.4	2232	239.5	661.8	4508.5	4091.2
294	At5g66540			666.8	4868.1	1058.1	4536.6	2298	5610.7
295	At2g42680	MBF1A	multiprotein bridging factor 1A	667.8	4455	1165.3	402	1578.9	1044
296	At5g17370	Transducin/W	Transducin/WD40 repeat-like superfamily protein	668.8	778.8	2074.7	8087.7	13718.4	7892.9
297	At2g31740	transferase	S-adenosyl-L-methionine-dependent methyltransferases superfamily protein	670.2	3236.3	431.6	5182.9	3547.8	3124
298	At1g14560	Mitochondria	Mitochondrial substrate carrier family protein	671.5	2954.1	133.5	5242.9	1211.5	3288.7
299	At5g64160			673.5	4855.8	508.6	690.4	4767.5	534.6
300	At1g51600	ZML2	ZIM-LIKE 2	676.3	1954	3680.7	1972.3	1181.2	9586.2
301	At5g55070	transferase	Dihydrolipoamide succinyltransferase	676.8	209.9	3665.6	1001.3	2781.4	3571.4
302	At4g01880	transferase	methyltransferases	678.9	5317.7	1010	2328.5	489.5	2652.2
303	At3g15660	GRX4	glutaredoxin 4	681.8	3753.9	891.2	481.6	2188.6	2122
304	At5g27660	Trypsin with	Trypsin family protein with PDZ domain	683.5	1580.2	1416.3	9378.7	4643.2	16089.4
305	At3g58180	ARM repeat	ARM repeat superfamily protein	683.6	5072.6	754.4	3683.1	1176.4	214.5
306	At1g54270	EIF4A-2	eif4a-2	684.6	7521	941.9	1301	2038.8	624
307	At2g40700	hydrolase	P-loop containing nucleoside triphosphate hydrolases superfamily protein	685.1	4967.2	794.9	2829.1	2502.1	12897
308	At5g14105			685.4	10085.5	717.9	599.1	840.5	292.4
309	263532_s_at		At2g24990;At5g37350	687.6	4536.5	921	2168.7	1779.5	1685.4
310	At2g43235			687.6	4287.3	928.7	1733.3	3615	20489.2
311	At5g09840	hydrolase	Putative endonuclease or glycosyl hydrolase	688.9	6525.5	427.9	6423.4	2625.3	5252.4
312	At5g20200	nucleoporin	nucleoporin-related	688.9	4079.5	1022.5	2859.4	3175.2	1013.4
313	At3g09720	hydrolase	P-loop containing nucleoside triphosphate hydrolases superfamily protein	689	6552.3	422.1	4694	2768.4	8056.5
314	At3g29010	ligase	Biotin/lipoate A/B protein ligase family	690.6	1594.5	1520	14144.4	7294.4	18241.5
315	At3g17240	mtLPD2	lipoamide dehydrogenase 2	694.5	638.9	6520.8	534	1067	761.2

	Locus	Alias	Function	MR(all)	MR(tissue)	MR(abiotic)	MR(biotic)	MR(hormone	MR(light)
316	At4g01320	STE24	Peptidase family M48 family protein	694.5	8353.5	280.4	587.5	2932.9	637.9
317	At1g29940	NRPA2	nuclear RNA polymerase A2	694.5	5915	891.4	2399.8	1994.3	2813.8
318	At1g20920	hydrolase	P-loop containing nucleoside triphosphate hydrolases superfamily protein	696.1	279	1218.5	6579	259	1714.9
319	At1g60650	RZ-1b	RNA-binding (RRM/RBD/RNP motifs) family protein with retrovirus zinc finger-like domai	698.3	3448.2	151.6	2911.8	2988.3	2710.2
320	At2g02090	ETL1	SNF2 domain-containing protein / helicase domain-containing protein	698.3	2847.7	2869.6	1167.5	164.4	16826.7
321	At3g19840	PRP40C	pre-mRNA-processing protein 40C	699	5571.2	177.6	4089.4	398.4	7199
322	At3g60360	UTP11	embryo sac development arrest 14	699	5749.9	275.1	3756.3	918.6	2372.8
323	At3g06480	helicase	DEAD box RNA helicase family protein	701.8	2812.4	1496.9	1999.2	2310.3	8012.1
324	At5g13030			702.7	1409.6	689.9	1287.3	513.4	1601.9
325	At5g12020	HSP17.6II	17.6 kDa class II heat shock protein	703	2278.3	604.1	3006.2	6346	15795.9
326	At1g71850	hydrolase	Ubiquitin carboxyl-terminal hydrolase family protein	705.3	6738.2	127.8	6181.3	4076.5	3163.3
327	At2g44510	inhibitor	CDK inhibitor P21 binding protein	705.7	8819.1	154.6	7906.1	12543.7	2276
328	At2g27285	DUF2040	Coiled-coil domain-containing protein 55 (DUF2040)	706.8	3606.6	873.7	258.1	8490.8	3976.8
329	At2g32600	glycoprotein	hydroxyproline-rich glycoprotein family protein	706.9	7311.2	407.4	775.5	1422	3387.3
330	At1g68370	ARG1	Chaperone DnaJ-domain superfamily protein	709.5	2271.4	1403.1	3369.7	1236.4	3854.3
331	At1g27050	homeobox 54	homeobox protein 54	710.2	4845	2157	4259.8	6160.8	2334.5
332	At5g17890	DAR4	DA1-related protein 4	712	1116.3	960.4	3522.4	1806.4	6289.1
333	At1g60080	nuclease	3'-5'-exoribonuclease family protein	713.1	5342	594.9	6291.2	6650.1	11063.1
334	At1g09300	M24	Metallopeptidase M24 family protein	714.5	1062.8	1549.1	2938.4	11698.7	6359.6
335	At3g02860	zinc ion bindi	zinc ion binding	714.8	1435.2	811.5	2928.8	5613.4	11444
336	At1g28060	splicing	Pre-mRNA-splicing factor 3	715	7607.9	172	2866.3	2663.3	2842.2
337	At4g18260	Cytochrome I	Cytochrome b561/ferric reductase transmembrane protein family	717.5	646.3	1238.6	5258.2	5515.1	4082.2
338	At1g56570	PGN	Tetratricopeptide repeat (TPR)-like superfamily protein	718.4	2346.3	6839.3	8359	294.6	9606
339	At1g10320	Zinc finger C-	Zinc finger C-x8-C-x5-C-x3-H type family protein	721.2	498.2	890.5	3922	12871.4	9136.2
340	At5g48970	Mitochondria	Mitochondrial substrate carrier family protein	723.3	4572.9	13.3	6887.1	1057.2	3025.7
341	At5g38830	tRNA syn	Cysteinyl-tRNA synthetase, class Ia family protein	725.5	7565.1	725.1	87.9	2914.9	3037.9
342	At5g14580	transferase	polyribonucleotide nucleotidyltransferase, putative	726	3186.7	980.4	4849.7	3864.6	5931.7
343	At5g19300			727.7	5551.1	932.3	2446.9	1301.7	5874.8
344	At5g41150	UVH1	Restriction endonuclease, type II-like superfamily protein	728.6	2929.5	1006.7	9170	566.6	5199.8
345	At4g32450	PPR	Pentatricopeptide repeat (PPR) superfamily protein	735.3	4234.4	135.5	11935.7	1745.5	16386.3
346	At4g04790	Tetratricopep	Tetratricopeptide repeat (TPR)-like superfamily protein	737.3	5447.5	334.7	3127.6	2188.3	9260.2
347	At2g34570	MEE21	PIN domain-like family protein	737.8	7316.7	604.3	6976.7	3302.1	3377.9
348	At1g53200			740.1	3582.6	265.9	4512.9	5230.8	3276.1
349	At5g47880	ERF1-1	eukaryotic release factor 1-1	742.1	5180.6	1634.5	714.9	3208.6	7143.8
350	At2g03270	DNA-binding	DNA-binding protein, putative	746	7296.7	892.2	1728.7	5359.3	10819
351	At2g39480	PGP6	P-glycoprotein 6	746.7	100.4	1612	2619.9	1542	3998.7
352	At4g30150			747.8	3215.4	848	4494	2310.4	2823.1
353	At5g44150			748.6	3907.5	696.6	2623.5	801.8	8855.3
354	At1g63070	PPR	pentatricopeptide (PPR) repeat-containing protein	751.2	8541.9	5146.1	11279	1041.9	13774.2
355	At3g03880	DUF1639	Protein of unknown function (DUF1639)	752.8	2567.1	1309.8	3134	17830.7	5242.1
356	At2g40780	OB-fold-like	Nucleic acid-binding, OB-fold-like protein	756.6	7440.8	744.8	3444.7	7970.6	20091.6
357	At2g16460	DUF1640	Protein of unknown function (DUF1640)	757.3	5796.8	415.6	1376.6	2732	2712.3
358	At1g78930	transcription	Mitochondrial transcription termination factor family protein	758.8	3493.4	68.7	12719.1	11244.6	1802.6
359	At3g53940	Mitochondria	Mitochondrial substrate carrier family protein	760.3	6787.9	44.3	12219.5	11376.5	11275.6
360	At2g04400	Aldolase-type	Aldolase-type TIM barrel family protein	763	607.6	2853.3	593.5	872.9	1510.8
361	At5g09390	CD2-binding	CD2-binding protein-related	765.6	4053.2	124.3	1445.6	2543.7	9779.8
362	At1g72560	PSD	ARM repeat superfamily protein	767.4	1168.2	549.7	13070.7	512.7	6948.3
363	At2g35733			768.4	3062	1189.6	9841.7	20942.7	8632.2
364	At5g11430	S-II	SPOC domain / Transcription elongation factor S-II protein	769.1	4339.1	2998.3	7002.4	8509.4	11487
365	266888_s_at		At1g02880;At2g44750	769.7	463	486.5	2865.1	6250.5	9693.1
366	At4g20010	PTAC9	plastid transcriptionally active 9	773.6	3358.5	2662.1	5034.9	1459.3	1089.8
367	At2g34160	DNA/RNA-bir	Alba DNA/RNA-binding protein	774.9	2094.9	815.9	2231.5	12329.5	5791.1
368	At1g06720	hydrolase	P-loop containing nucleoside triphosphate hydrolases superfamily protein	775.9	5694.9	802.7	3171	1452	5624.3
369	At5g53440			781.8	2222.5	1123.5	1535.8	1312	8726.7
370	At5g49400	CCHC-type	zinc knuckle (CCHC-type) family protein	784.8	2151.5	3551.8	782.2	721.5	5403.8
371	At1g75200	SAM	flavodoxin family protein / radical SAM domain-containing protein	788.4	8767.6	874.3	3038	4262.2	232.4
372	At4g15850	RH1	RNA helicase 1	791.4	4062	341.8	5415.6	2496.5	19987.2
373	At3g27700	RRM	zinc finger (CCCH-type) family protein / RNA recognition motif (RRM)-containing protein	793	355	2124.6	2853.4	6558	7130.7
374	254593_s_at		At4g18900;At4g18905	793.3	1357.5	1362.7	4989.9	2749.3	4573.5
375	At5g53770	transferase	Nucleotidyltransferase family protein	793.7	6785.2	509.1	8926.7	204.4	5360.1
376	At1g03860	PHB2	prohibitin 2	795	7701.1	445.4	3027.6	1472	587.9
377	At5g23710	RNA polymer	DNA binding;DNA-directed RNA polymerases	796.4	4568.9	1098.7	1911	17029.1	3982.2
378	At3g27550	CRM	RNA-binding CRS1 / YhbY (CRM) domain protein	797.6	4586.1	53.4	4468.6	14747.4	4533.8
379	At1g17680	TPR	tetratricopeptide repeat (TPR)-containing protein	800.9	877.4	1744.2	1011.7	3853.8	3672.3
380	At1g47870	E2FC	winged-helix DNA-binding transcription factor family protein	801.4	7170.8	947.4	799.9	1318.5	8435.4
381	258259_s_at		At3g26820;At3g26840	803.6	1705.1	552.7	434.8	2936.4	8497.1
382	At3g05090	LRS1	Transducin/WD40 repeat-like superfamily protein	804.7	1275.2	1209.8	661.1	1097.8	2746.5
383	At5g52200	I-2	phosphoprotein phosphatase inhibitors	805.4	2738.1	4506.7	909.6	6389.4	7484.5
384	At3g03420	Ku70-binding	Ku70-binding family protein	806.6	8472.3	197.4	3776.3	4555.5	1728.9
385	266389_s_at		At2g31580;At2g32320	806.9	81.1	1378.2	1142.3	4375.5	2172.3
386	At3g04130	Tetratricopep	Tetratricopeptide repeat (TPR)-like superfamily protein	809	2384	267.3	5292	4757.9	11128.5
387	At5g63690	OB-fold-like	Nucleic acid-binding, OB-fold-like protein	809.3	1050.9	1291.9	5546.4	4130.3	15384.4
388	At5g13310			810.1	3631.5	1618.3	636.2	6606.5	6468.3
389	At1g80950	transferase	Phospholipid/glycerol acyltransferase family protein	811	3886.8	6968.6	1680.2	1836.4	7166.7
390	At5g14950	GMII	golgi alpha-mannosidase II	811.9	818.2	5102.7	664.6	778.2	3252.6
391	At5g11240	transducin	transducin family protein / WD-40 repeat family protein	813.1	8808.1	384.1	3979.4	5044.7	939.4
392	253415_at			813.4	4435.9	207.9	2094.3	892.5	16102.5
393	At4g32050	neurochondr	neurochondrin family protein	815.1	4924.9	343.3	8947.9	8803	13057.4
394	At5g67080	MAPKKK19	mitogen-activated protein kinase kinase kinase 19	815.3	1919.2	4467.5	1437.7	1866.8	13329.5

	Locus	Alias	Function	MR(all)	MR(tissue)	MR(abiotic)	MR(biotic)	MR(hormone	MR(light)
395	At2g44820			816.7	3907	2497.3	4177.1	2599.2	10552
396	At1g62740	Hop2	stress-inducible protein, putative	817.7	7043.9	1392.6	3154.1	90.9	13865.1
397	At1g15420			818.7	8420.8	118.5	9290.9	2713	883.8
398	At4g12750	transcription	Homeodomain-like transcriptional regulator	824.2	3946.9	1007.4	6490.5	4808.4	2504.9
399	At5g58020			826	6349.1	26.5	1443.2	14785.1	1402.4
400	At1g76170	TtcA	2-thiocytidine tRNA biosynthesis protein, TtcA	827.8	2290.4	1115	16047.4	10778.2	10639.1
401	At3g16840	hydrolase	P-loop containing nucleoside triphosphate hydrolases superfamily protein	830.9	7339.1	994.9	4835.7	360.9	2412.3
402	267162_s_at		At2g05140;At2g37690	832.1	4113.5	953.5	4214.9	2992.3	1574.5
403	At4g25730	transferase	FtsJ-like methyltransferase family protein	833.1	8110.4	560.6	2189.1	1610.4	114.1
404	At3g06940	transposable	transposable element gene	835.3	995.8	1838.4	562.6	4205.9	7637.2
405	At3g62450			836.4	4789.2	2273.9	660.4	2742.9	2202.2
406	At3g60980	Tetratricopep	Tetratricopeptide repeat (TPR)-like superfamily protein	836.8	1300	1951.7	4941.7	1670.5	5667.6
407	At1g09190	Tetratricopep	Tetratricopeptide repeat (TPR)-like superfamily protein	837.3	1684.2	2822.9	6284.4	5505.2	11456.7
408	At4g32430	PPR	Pentatricopeptide repeat (PPR) superfamily protein	839	1476.2	970	8881.5	10268.4	5686.3
409	At4g24820	PCI	26S proteasome, regulatory subunit Rpn7;Proteasome component (PCI) domain	839.3	9760.4	576	411.5	4238.6	342
410	249616_s_at		At5g37440;At5g37750	840.5	3613.7	347.8	4366.2	14861	673.9
411	At4g02560	LD	Homeodomain-like superfamily protein	842.3	3513.5	489	2274.3	560.9	11051.4
412	At5g65850	F-box	F-box and associated interaction domains-containing protein	842.5	4682.3	214.2	3672.2	9236.9	8707.3
413	At5g10630	IF2gamma	Translation elongation factor EF1A/initiation factor IF2gamma family protein	842.8	6706	764.8	10859.8	3322.5	3912.1
414	At1g11780	oxygenase	oxidoreductase, 2OG-Fe(II) oxygenase family protein	844.4	3058.3	3122.5	15533.9	544.6	7914.3
415	At2g34357	ARM repeat	ARM repeat superfamily protein	845.2	7898.6	895.2	4039.7	1428.8	3632.1
416	At1g07840	Sas10	Sas10/Utp3/C1D family	846.2	10886	1349.4	6299.2	2111	8411
417	At1g11800	phosphatase	endonuclease/exonuclease/phosphatase family protein	848.5	11441.5	197.7	6702.6	11064.8	4654.3
418	262227_s_at		At1g53750;At1g53780	848.9	3950.7	2052	295.8	1953.7	1038.1
419	At1g48040	Protein phos	Protein phosphatase 2C family protein	854.1	3936.7	952.6	2855.5	3432.5	18131.6
420	At1g29220	transcription	transcriptional regulator family protein	854.7	2383.1	882.2	1906.5	14066.8	8382.6
421	At3g23620	Ribosomal RN	Ribosomal RNA processing Brix domain protein	856.5	9437.3	336	3905.5	4400.3	1544.7
422	At5g39840	helicase	ATP-dependent RNA helicase, mitochondrial, putative	859.5	6193.3	724.9	7303.2	1739.1	6563.9
423	At3g10650	NUP1		861.1	2694.8	742.6	3793.7	1566.8	6691.7
424	255093_s_at		At4g08580;At5g17900	861.8	2708.6	392.7	1444.6	268.5	10849.7
425	At2g34780	MEE22	maternal effect embryo arrest 22	861.9	6305.5	490	11377.8	3726.4	2886.4
426	At1g15440	PWP2	periodic tryptophan protein 2	862.8	8173.7	465.4	4717.5	4576.9	382.3
427	At4g25340	FKBP53	FK506 BINDING PROTEIN 53	863.2	8988.5	497.5	2625.2	3740.9	5138.8
428	At4g03230	kinase	S-locus lectin protein kinase family protein	864.5	4268.8	495	6174.8	2685.6	12908.4
429	At5g57280	RID2	S-adenosyl-L-methionine-dependent methyltransferases superfamily protein	865	8319.6	677.7	3391.8	2110.7	1592.3
430	At5g16860	Tetratricopep	Tetratricopeptide repeat (TPR)-like superfamily protein	867.1	5908.9	1170.3	7258.8	2927.6	2683.7
431	At5g11520	YLS4	aspartate aminotransferase 3	872.9	1837.4	3228.4	419.5	2221.9	1627.7
432	At1g32530	RING	RING/U-box superfamily protein	874.5	2586.8	317.4	461.4	2720.9	5827.7
433	At2g02730	DUF1664	Protein of unknown function (DUF1664)	874.8	998.8	417	1611.2	8880	16585
434	At4g10710	SPT16	global transcription factor C	879.8	2474.3	1584.8	1243.1	1358.8	6318.9
435	At3g28210	SAP12	zinc finger (AN1-like) family protein	880.5	4464.5	1064.1	2030.7	6061.4	11843.9
436	At1g09290			886.6	3264.7	1882.1	9326.4	5128.2	8203.5
437	AtMg00510	NAD7	NADH dehydrogenase subunit 7	886.7	3271.6	1473.1	2328	1337.4	14686.2
438	At5g14440	SURF2	Surfeit locus protein 2 (SURF2)	893.2	7924.3	1901.2	3052.3	1808.1	3259
439	At1g55500	ECT4	evolutionarily conserved C-terminal region 4	895	1669.1	1474.2	3981.9	1919.6	1812.1
440	At3g19360	CCCH-type	Zinc finger (CCCH-type) family protein	895.6	7659.5	313.4	4968.9	4597.7	1590.9
441	At4g23910			896.1	6108.5	331.4	8779.6	7978.9	9145.5
442	At4g32240			898	5620.9	834.9	6710.7	6879.2	1906.8
443	At2g47410	WD40	WD40/YVTN repeat-like-containing domain;Bromodomain	900.3	308.5	1064.5	2879.3	859.9	4847.5
444	257320_at			901.9	658.1	858.5	6402.5	15094.7	16633.6
445	248743_at			905.1	7192	299.6	2821.8	4065.5	2845.9
446	At1g79540	PPR	Pentatricopeptide repeat (PPR) superfamily protein	906.7	3301.7	963.1	5519.9	13151.6	2281.2
447	At2g18900	Transducin/W	Transducin/WD40 repeat-like superfamily protein	908.6	4545.4	790.7	4603.2	6148.2	948.3
448	At1g56350	Peptide chair	Peptide chain release factor 2	911.6	2738.1	2253	4342.7	4594.7	7960.9
449	At5g12190	RNA-binding	RNA-binding (RRM/RBD/RNP motifs) family protein	912.4	7945.5	1107.3	1306.5	8207.8	907.1
450	At3g46460	UBC13	ubiquitin-conjugating enzyme 13	914.1	8453.4	855.2	6890.2	1563.6	4182.8
451	265941_s_at		At2g19490;At3g32920	914.9	4446.7	751	4587	3934.8	4057.1
452	At1g16010	MRS2-1	magnesium transporter 2	915.5	1080.7	862.1	6542.4	1512	6291.3
453	At1g23280	MAK16	MAK16 protein-related	916	8223.7	231.4	5066.4	1832	5831.1
454	At1g29150	RPN6	non-ATPase subunit 9	916.6	8423.5	1379.6	831.8	4486.7	3968.1
455	At2g30800	HVT1	helicase in vascular tissue and tapetum	919	3175.1	347.5	2583.4	150.2	389.9
456	At1g55040	Ran-binding	zinc finger (Ran-binding) family protein	919.5	2127.5	8721.3	2358.4	3090.7	14551.8
457	At1g64600	transferase	methyltransferases;copper ion binding	921	3499.5	486.4	3712.7	11142.4	14848.9
458	At5g45140	NRPC2	nuclear RNA polymerase C2	921.9	3893.1	289.2	7750.9	1574.5	16124.4
459	At5g14250	FUS11	Proteasome component (PCI) domain protein	925.8	6490.6	433.8	2824.3	2269	7371.4
460	At5g62910	RING	RING/U-box superfamily protein	933	3279.4	1198.2	992.7	4242.5	5079.1
461	At2g40430			933.7	7856.7	1284.2	1941	917.3	4132.2
462	At4g19610	nucleotide bi	nucleotide binding;nucleic acid binding;RNA binding	934.3	8477.7	603	6419.3	353.4	4203.6
463	At5g67440	NPY3	Phototropic-responsive NPH3 family protein	935.3	166.3	6363.5	5493.1	5413.4	22549.4
464	At3g59630	DPH2	diphthamide synthesis DPH2 family protein	937.4	3415.8	1905.2	5038.5	2876.5	2787.6
465	At3g06720	IMPA1	importin alpha isoform 1	938.3	5376.1	759	2030.3	3991	10886.5
466	At3g22170	FHY3	far-red elongated hypocotyls 3	940.6	1338.7	636	1003	1358.8	3721.6
467	At1g51310	transferase	transferases;tRNA (5-methylaminomethyl-2-thiouridylate)-methyltransferases	941.6	3480	75.1	15258.2	3551.2	3162.8
468	At5g35680	OB-fold-like	Nucleic acid-binding, OB-fold-like protein	941.8	5644.2	2361.9	1342.5	15807.6	960.9
469	253596_s_at		At4g30730;At4g30750	941.9	5529.2	1076.4	97	2154.2	2248
470	At4g28600	NPGR2	no pollen germination related 2	946.9	9882.2	764.8	547.6	1319.2	1629.2
471	At5g39040	TAP2	transporter associated with antigen processing protein 2	947.2	10194.5	1154.4	3498.3	166.7	3367.6
472	At3g10530	Transducin/W	Transducin/WD40 repeat-like superfamily protein	948.5	6910.3	401.6	5152	4553	3165.8
473	At4g14850	MEF11	Pentatricopeptide repeat (PPR) superfamily protein	950.8	2415.2	943.4	4755.3	11591.1	12434.2

	Locus	Alias	Function	MR(all)	MR(tissue)	MR(abiotic)	MR(biotic)	MR(hormone	MR(light)
474	At3g04800	TIM23-3	translocase inner membrane subunit 23-3	951	2331.7	9468.8	13694.3	17096	8353.7
475	At1g26340	CB5-A	cytochrome B5 isoform A	952.7	10515.5	936.7	1789.1	8643.5	5357.2
476	At5g50840			953	6703.9	2911.1	1773.4	1208.2	6337.4
477	At1g30070	SGS	SGS domain-containing protein	953.9	2727.2	2056.7	3628.2	2066.5	20230.1
478	At3g01160			954.4	10862.6	252	3437.3	3062.4	2871.7
479	At5g53800			955.2	2797.8	647.2	1132	2171.9	8802.6
480	259937_s_at		At1g71330;At3g13080	957.4	172.3	1868.2	3000.7	3901.7	904.2
481	At2g43650	Sas10	Sas10/U3 ribonucleoprotein (Utp) family protein	959.8	8475.7	551.4	8622.5	1529.5	5000.3
482	At5g46680	PPR-like	Pentatricopeptide repeat (PPR-like) superfamily protein	960.1	1070.3	979.1	8715.7	17474.2	15906.9
483	At3g13330	PA200	proteasome activating protein 200	960.9	5218.6	5342.1	593	204.8	992.4
484	At4g04940	transducin	transducin family protein / WD-40 repeat family protein	963.9	7807.5	880.5	3680.3	5160.4	1058.9
485	At5g65720	NIFS1	nitrogen fixation S (NIFS)-like 1	964.9	1575.5	3341.9	2866.9	3326.6	7118.8
486	At5g37370	SRL1	PRP38 family protein	969.7	198.4	4453	203	2494.4	12497.3
487	At5g60590	DHBP syntha	DHBP synthase RibB-like alpha/beta domain	970.4	62.2	3469.5	4842.4	3307.7	6367.6
488	At1g80550	PPR	Pentatricopeptide repeat (PPR) superfamily protein	972.9	2789.7	359.4	6739.1	4377.1	12173.6
489	267229_s_at		At2g44070;At5g38640	974.3	6219.1	2658.4	2650.2	131.2	10273.2
490	262306_s_at		At1g70980;At5g56680	975.1	9957.1	898.1	1794.4	1993	322.4
491	248517_at		At5g50550;At5g50650	979.1	2618.6	4745.6	3983	4128.9	4491.9
492	At1g49880	Erv1	Erv1/Alr family protein	979.8	1631.4	3230.5	10079.3	5078	21122.1
493	At1g16280	SWA3	RNA helicase 36	980.8	7343.6	344.6	8251.6	4492.5	5168.2
494	At3g52220			982.4	448.2	4037.6	2015.8	639.1	4210.4
495	At1g77840	IF2/IF5	Translation initiation factor IF2/IF5	985.8	10187.1	383	780.6	1190.5	1586.8
496	At4g37670	NAGS2	N-acetyl-l-glutamate synthase 2	987.1	4161.9	6492.4	1285.7	191.6	20622.9
497	At3g54980	PPR	Pentatricopeptide repeat (PPR) superfamily protein	989.1	4436.6	1053.6	5079.1	2199.4	422.2
498	At5g52070	Agenet	Agenet domain-containing protein	992.3	217.6	1446	961.9	4848.8	18634.2
499	At1g20575	DPMS1	Nucleotide-diphospho-sugar transferases superfamily protein	992.5	8115.5	679.7	276.6	2161.6	6273.5
500	At5g13750	ZIFL1	zinc induced facilitator-like 1	993.7	2985.3	1242.3	1377.4	3871.8	3490.4